

12

NWC TP 6288

Survivability Analysis for Impacting Warheads With Shear-Control Grids

by
Olaf E. R. Heimdahl
and
John Pearson
Research Department

FEBRUARY 1982

**NAVAL WEAPONS CENTER
CHINA LAKE, CALIFORNIA 93555**



Approved for public release; distribution unlimited.

S DTIC ELECTE D
JUL 12 1982
B

82 07 12 026

AD A116795

DTIC FILE COPY

Naval Weapons Center

AN ACTIVITY OF THE NAVAL MATERIAL COMMAND

FOREWORD

The research described in this report was conducted in support of controlled fragmentation studies for hard target penetrator warheads under the Air Strike Warfare Weaponry Technology Block Program at the Naval Weapons Center. The work was performed during Fiscal Year 1981, and was funded by AIRTASK WF 32395, Program Element 62332N, Work Unit 1321051.

This report was reviewed for technical accuracy by W. J. Stronge.

Approved by
E. B. ROYCE, *Head*
Research Department
15 December 1981

Under authority of
J. J. LAHR
Capt., U.S. Navy
Commander

Released for publication by
R. M. HILLYER
Technical Director

NWC Technical Publication 6288

Published by.....Technical Information Department
Collation.....Cover, 21 leaves
First printing.....150 unnumbered copies

UNCLASSIFIED

SECURITY CLASSIFICATION OF THIS PAGE (When Data Entered)

REPORT DOCUMENTATION PAGE		READ INSTRUCTIONS BEFORE COMPLETING FORM
1. REPORT NUMBER NWC TP 6288	2. GOVT ACCESSION NO. AD-A116795	3. RECIPIENT'S CATALOG NUMBER
4. TITLE (and Subtitle) SURVIVABILITY ANALYSIS FOR IMPACTING WARHEADS WITH SHEAR-CONTROL GRIDS	5. TYPE OF REPORT & PERIOD COVERED Research report Fiscal Year 1981	
	6. PERFORMING ORG. REPORT NUMBER	
7. AUTHOR(s) Olaf E. R. Heimdahl and John Pearson	8. CONTRACT OR GRANT NUMBER(s)	
9. PERFORMING ORGANIZATION NAME AND ADDRESS Naval Weapons Center China Lake, CA 93555	10. PROGRAM ELEMENT, PROJECT, TASK AREA & WORK UNIT NUMBERS AIRTASK WF 32395, 62332N, Work Unit 1321051	
11. CONTROLLING OFFICE NAME AND ADDRESS Naval Weapons Center China Lake, CA 93555	12. REPORT DATE February 1982	
	13. NUMBER OF PAGES 40	
14. MONITORING AGENCY NAME & ADDRESS (if different from Controlling Office)	15. SECURITY CLASS. (of this report) UNCLASSIFIED	
	15a. DECLASSIFICATION/DOWNGRADING SCHEDULE	
16. DISTRIBUTION STATEMENT (of this Report) Approved for public release; distribution unlimited.		
17. DISTRIBUTION STATEMENT (of the abstract entered in Block 20, if different from Report)		
18. SUPPLEMENTARY NOTES		
19. KEY WORDS (Continue on reverse side if necessary and identify by block number)		
Terminal ballistics Warhead survivability Fragmentation control Impact	Stresses Finite element Computer Analysis (numeric)	Stress raisers Response Deformation Dynamic plasticity
20. ABSTRACT (Continue on reverse side if necessary and identify by block number) See back of form.		

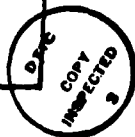
UNCLASSIFIED

SECURITY CLASSIFICATION OF THIS PAGE(When Data Entered)

(U) *Survivability Analysis for Impacting Warheads With Shear-Control Grids*, by Olaf E. R. Heimdahl and John Pearson. China Lake, Calif., Naval Weapons Center, February 1982. 40 pp. (NWC TP 6288, publication UNCLASSIFIED.)

(U) Pearson's shear control method of fragmentation control has been successfully employed in a variety of bombs and warheads and has potential application for impacting warheads. In this study we have investigated the response of a grooved warhead case to impact loads by using the finite element code HONDO II. The characteristic response of the case segment containing the groove is the appearance of two linearly shaped regions of yielding emanating from the groove location. The effect of a shear-control grid on the survivability of a warhead depends on the grid location and on the groove depth.

Accession For	
NTIS GRA&I	<input checked="" type="checkbox"/>
DTIC TAB	<input type="checkbox"/>
Unannounced	<input type="checkbox"/>
Justification	
By	
Distribution/	
Availability Codes	
Dist	Avail and/or Special
A	



UNCLASSIFIED

SECURITY CLASSIFICATION OF THIS PAGE(When Data Entered)

CONTENTS

Introduction	3
The Use of Shear-Control Grids	4
Area of Application	4
Grid Pattern	5
Grid Profile Configurations	5
Material Properties	7
Failure of Impacting Warheads	7
Warheads Without Grid Systems	7
Penetrating Concrete	8
Perforating Steel	8
Warheads With Grid Systems	9
Survivability Study	9
Scope of Study	9
Assumptions	10
Method of Analysis	11
Warhead Models	11
Case Segment Models	14
Results of the Case Segment Analysis	14
Groove Configuration	14
Groove Location	16
Depth of the Groove	25
Growth of the Bands of Yielding	26
Case Deformations	30
Discussion and Conclusions	34
Reduction in Energy Absorption Capacity	34
Secondary Failure Zone	35
Ductile Fracture	35
Brittle Fracture	36
Experimental Evidence	36
Summary	37

Figures:

1. Fracture and Control Zones	4
2. Shear-Control Grid in Warhead Case	6
3. Fracture Trajectories for Grid Element Profiles	6
4. Projectile Deformation Due to Penetration of Concrete	8
5. Projectile Deformation Due to Perforation of Steel Plate	9
6. Circumferential Groove Replacing Complete Shear-Control Grid System for Purpose of Analysis	10
7. Finite Element Models of Warhead With and Without Circumferential Groove	12
8. Regions of Yielding for Grooved and Plain-Wall Warheads Impacting a Steel Plate	13
9. Finite Element Model of Grooved and Plain-Wall Case Segments	15
10. Pressure Versus Time Curves Applied to Test Specimens of Case Segments	16
11. Regions of Yielding (a) Plain-Wall Cylinder	17
(b) Grooved Cylinder	19
12. Regions of Yielding for Grooved Case Segments	21
13. Finite Element Models for Extended Test Case Segments	22
14. Regions of Yielding for Extended Test Case Segments Showing Maximum Extensions of Region	23
15. Regions of Yielding for Extended Test Case Segment Under Longer Load Duration Showing Maximum Extension	24
16. Zones of Yielding in Shallow "Vee" Grooved Segment	26
17. Finite Element Model of Case Segment With .75-inch Wall Thickness	27
18. Regions of Yielding for Extra-Wide Case Segment	28
19. Extent of Radial Yielding Region From Notch	29
20. Plain-Wall Case Segment Deformation	31
21. Grooved Case Segment Deformation	32
22. Grooved Case Segment, Groove on Outer Surface, Deforming	33

Tables:

1. Steels Used in Shear-Control Studies at NWC	7
--	---

INTRODUCTION

There is a recognized need for fragmentation control methods for the warheads of penetrator weapons that are to be used against moderately hard and hard targets. One possible approach is the shear-control method of fragmentation.^{1,2} This method could be considered for use provided a control grid were compatible with both the material properties of the case and the design requirements of the warhead. Since, however, a shear-control grid machined or formed into the inner surface of the warhead case may act as a stress raiser during target interaction, it is necessary to determine if the presence of such a grid would affect the structural integrity of the warhead case and, hence, the survivability of the weapon during the impact and penetration process.

In the present study, an investigation of the likely effects of a shear-control grid on the survivability of a blunt-nosed warhead impacting a moderately hard target was made through the use of a two-dimensional finite element code, HONDO II.³ For an expedient analysis, grid effects were modeled by means of circumferential grooves on the inside surface of the warhead case. While this groove geometry was used primarily to meet the requirements of the HONDO II code, it also appeared, based on the work of Stronge and Schulz on the failure modes of normally impacting penetrators,⁴ to be a simple way to model an extreme stress-raiser geometry relative to the use of this fragmentation control method. The study considered survivability effects due to groove location and the cross-sectional configuration and orientation of the groove profile.

¹ Naval Weapons Center. *Parametric Studies for Fragmentation Warheads*, by John Pearson. China Lake, Calif., NWC, April 1968. (NWC TP 4507, publication UNCLASSIFIED.)

² John Pearson. "The Shear-Control Method of Warhead Fragmentation," in *Fourth International Symposium on Ballistics, Monterey, Calif., October 1978*. Monterey, Calif., NPS, 1978. (Publication UNCLASSIFIED.)

³ Sandia Laboratories. *HONDO II, a Finite Element Computer Program for the Large Deformation Dynamic Response of Axisymmetric Solids*, by S. W. Key, Z. E. Beisinger, and R. D. Krieg. Albuquerque, New Mexico, Sandia Labs., 1978. (SAND78-0422, publication UNCLASSIFIED.)

⁴ W. J. Stronge and J. C. Schulz. "Projectile Impact Damage Analysis," *J. Computers and Structures*, Vol. 13, No. 1-2 (1981), pp. 287-294.

THE USE OF SHEAR-CONTROL GRIDS

AREA OF APPLICATION

Most fragmentation control methods are intimately related to the modes of energy absorption that are present in the metal during the fragmentation of the warhead case. For example, the effectiveness of the method may depend on whether the warhead case normally fragments primarily by means of shear or tensile breaks. To be most effective, the control method should utilize the stress system generated in the warhead case during the initial phase of case expansion so as to enhance the natural fragmentation behavior of the metal along definite and pre-determined paths. Accordingly, the shear-control method of fragmentation is most effective when used with a warhead that has case material properties and case dimensions such that shear fracture predominates in the fragmentation process.

The diagram of Figure 1 indicates in a general way how wall thickness relates to the relative zones of fracture behavior, and the approximate regions for which different types of fragmentation control methods

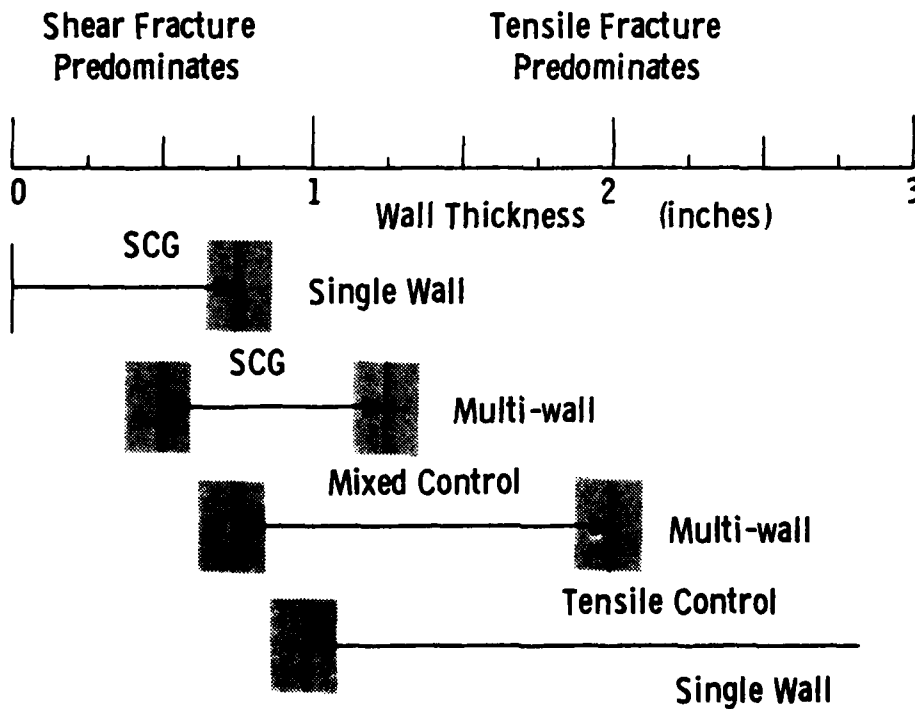


FIGURE 1. Fracture and Control Zones. (SCG = Shear Control Grid.)

should be effective, for warheads in the 10- to 12-inch-diameter range with a case made of a ductile, high-strength steel. As shown in the figure, as the case thickness for a given size warhead is increased, the predominant mode of fracture changes from shear to tensile, and different types of fragmentation control systems are required. Also, as the wall thickness is increased, the desired fragment size may require consideration of a multi-wall design and even the possible use of a mixed control scheme. In applying the concept of Figure 1, which is to match the control method to the predominant mode of fracture, it should be recognized that quantitative values for defining both the fracture zones and the control regions will vary with the properties of the case material, the charge-mass ratio of the warhead, and very strongly on a judgmental basis of what is an acceptable fragmentation signature for a given warhead.

The left side of the diagram shows the approximate range where a shear-control grid can be used effectively with a single-wall case. A number of the warheads for projected penetrator weapons also fit into this region of control, and it is for this area of application that this investigation was conducted.

GRID PATTERN

The shear-control method of warhead fragmentation uses families of mechanical stress raisers in the form of a grid system that is usually machined or formed into the inner surface of the warhead case. The elements of the grid system control the initiations of shear fractures at the root of each grid element, and the shear fractures then propagate along fracture trajectories established by the stress field existing in the warhead case during the initial phase of case expansion. The control grid is designed to match the geometry of this stress field and to utilize the principal strains in the metal to activate only specific families of fracture trajectories and thus produce fragments of a predetermined size and shape. For cylindrical warheads, the most commonly used grid design is a diamond pattern, with the diamonds elongated in the axial direction, as shown in Figure 2. Such a pattern makes effective use of the strain field generated in the expanding case, and also produces fragments of a desirable shape and size.

GRID PROFILE CONFIGURATIONS

The grid profile configuration is the cross-sectional shape of the individual grid elements. In general, the grid element profile is given by one of two basic shapes; it is either symmetrical or nonsymmetrical as shown in Figure 3. The shear trajectories that represent the possible paths of shear fracture propagation emanate in mutually orthogonal pairs from the root of each element in the grid system. Whether the controlled fractures tend to propagate along both trajectories, or are restricted to



FIGURE 2. Shear-Control Grid in Warhead Case.

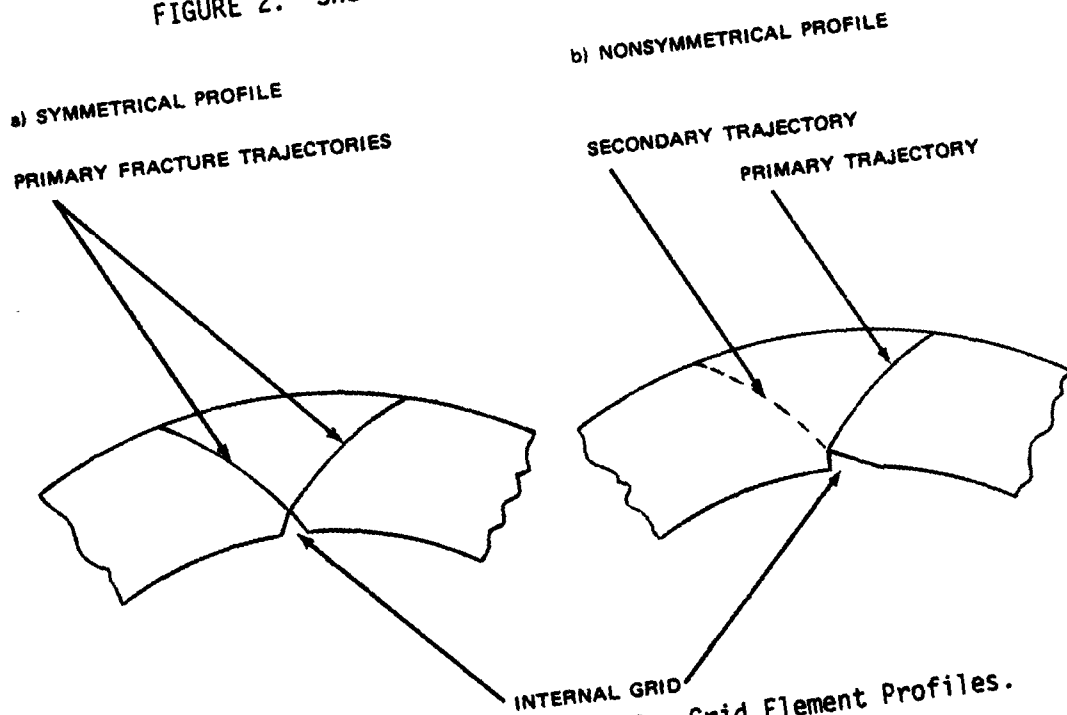


FIGURE 3. Fracture Trajectories for Grid Element Profiles.

only certain trajectories of a specific orientation is governed by the cross-sectional profile of the grid. For a symmetrical profile (Figure 3a), both trajectories support fracture to the same degree, while for a non-symmetrical profile (Figure 3b), the primary trajectory supports fracture to a much greater degree than does the secondary trajectory.

MATERIAL PROPERTIES

One of the most important factors in the use of the shear-control method is the behavioral property of the case material. Since this control method is based on controlled shear fracturing, the method works best when used with ductile steels, and is least effective with brittle steels. If the warhead case fractures completely through the wall in shear, or if shear fracture occurs through most of the wall, then that case should work well with this method for a warhead of that size. If, on the other hand, the case fractures predominantly in tension, it is generally not suited to this type of control.

Table 1 lists a number of different steels that have been studied at the Naval Weapons Center (NWC) for appropriateness of use with the shear-control method.¹ A general guide, based on these studies, indicates that most of these steels should be generally acceptable at least up to a hardness value of about Rockwell C 40. It should be noted that a number of the high-strength, heat-treatable steels that were fully acceptable for use with this control method would also be candidate materials for penetrator warheads.

TABLE 1. Steels Used in Shear-Control Studies at NWC.

Type	Hardness, Rockwell	Ultimate strength, psi	Suitability
SAE 1015...	B 75	65,000	Acceptable
SAE 1026...	B 95	100,000	Acceptable
SAE 1040...	C 22	110,000	Acceptable
SAE 4142...	C 22	118,000	Acceptable
AISI 52100.	C 28	120,000	Acceptable
SAE 4340...	C 31	155,000	Acceptable
Hy Tuf.....	C 40	190,000	Acceptable
AISI 52100.	C 46	237,000	Marginal
AISI 52100.	C 60	310,000	Too brittle

FAILURE OF IMPACTING WARHEADS

WARHEADS WITHOUT GRID SYSTEMS

In order to assess the effect that a shear-control grid may have on the failure of an impacting warhead, it is first necessary to understand the general failure mode of the warhead without a grid system. It is then possible to fairly evaluate the probable effects that the addition

of a grid system could have on warhead survivability. Analysis by finite element and experimental firings of smooth-cavities test projectiles⁴ demonstrate two basic deformation patterns and failure modes for normally impacting warheads, depending on the type of target.

Penetrating Concrete

The projectile penetration of thick concrete targets produces moderately severe loads of long duration, which result in a pronounced cavity bulge illustrated in Figure 4. While there is significant deformation at the front end of the warhead, the greatest strains are experienced in the region of the cavity bulge, which is referred to as the primary failure zone of the warhead. For impact velocities greater than a characteristic value for the specific warhead, a critical strain is exceeded in the primary failure zone and the material fails in shear, resulting in breakup of the projectile and termination of the penetration. It appears that the introduction of stress raisers in the primary zone of failure (such as the grooves of a shear-control grid) could significantly reduce the critical impact velocity at which the warhead fails.

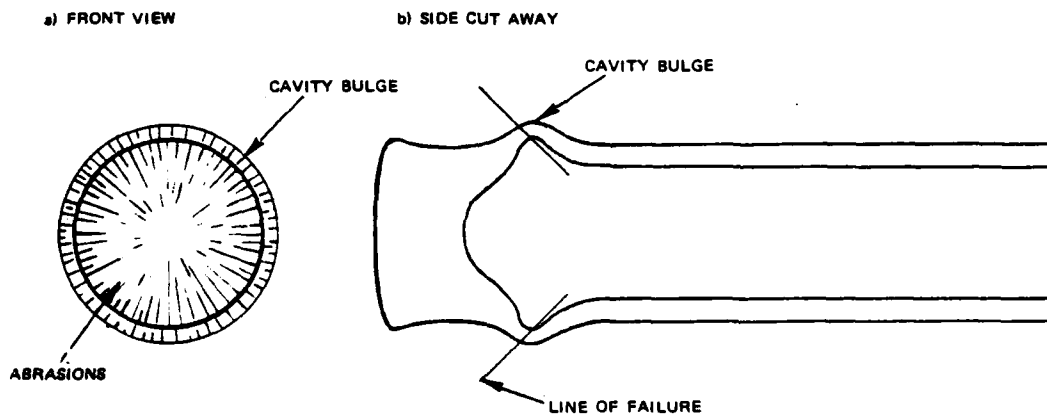


FIGURE 4. Projectile Deformation Due to Penetration of Concrete.

Perforating Steel

Perforation of a steel plate target results in a high load of short duration on the front end of the warhead as a disk is plugged from the target. The resulting deformation (Figure 5) is largely confined to mushrooming of the front end, with bulging also occurring in the same primary zone of failure. Projectile breakups depend on projectile striking velocity and target thickness. Radial fractures, plugging, multiple spalling, and even complete shattering of the nose plate may occur, depending on impact velocity. Since the damage to the warhead is concentrated at the

front end of the warhead, the case need not be as thick as for a case designed to go against a semi-infinite concrete target. The effect of a shear-control grid would depend on the case thickness. If the case were thin enough so that the cavity bulge became the primary failure region, then the presence of this stress raiser could be important.

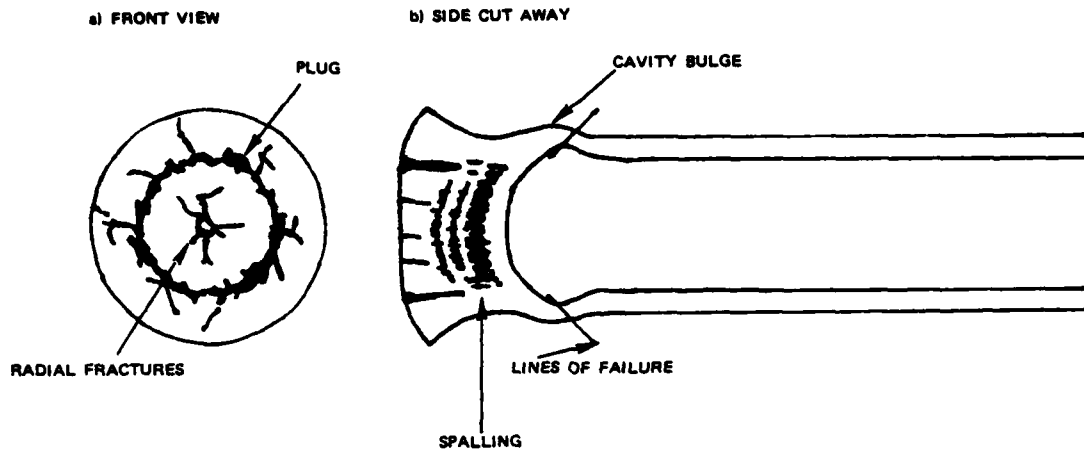


FIGURE 5. Projectile Deformation Due to Perforation of Steel Plate.

WARHEADS WITH GRID SYSTEMS

The presence of stress concentrators, such as notches, holes, welds, and joints, generally weakens a structure and reduces its capacity to absorb energy and survive impulsive loading. Since fragment control by use of a grid system purposefully introduces dynamic stress raisers, it could be anticipated that the use of a fragment-control grid system might reduce the survival velocities of an impacting warhead, depending on the warhead design and target characteristics. The response of a grid system to dynamic compressive loads needs to be studied to show the differences between the stress patterns and the resulting deformations for the scored case versus the smooth case, and to find how the design elements of a grid system affect the response to these loads.

SURVIVABILITY STUDY

SCOPE OF STUDY

The purpose of this study was to investigate the possible effects of shear-control grooves on the survivability of impacting warheads. The main tool in this investigation was a two-dimensional finite element code,

called HONDO II. Since the code is limited to axisymmetric bodies, this analysis was restricted to circumferential grooves and impacts of normal obliquity. The study of longitudinal grooves, complete grid systems, or oblique impacts would necessitate either an experimental investigation or a three-dimensional analysis. The study analyzed the effects of a circumferential groove and offers the conclusions as representative for the effects that would be produced by a full grid system. Simplification of the problem to a single circumferential groove (Figure 6) aligns the plane of the groove with the plane in which non-grooved warheads are most likely to fail and places this stress raiser as near to the load as possible. It is expected that if a warhead with a complete grid system were to fail due to the presence of the grid pattern, the failure would start in the portion of the grid nearest the front end of the warhead, or in the primary failure zone. Thus, the study of warheads with a single circumferential groove should provide a good basis for drawing conclusions as to how shear-control grids affect the survivability of normally impacting warheads.

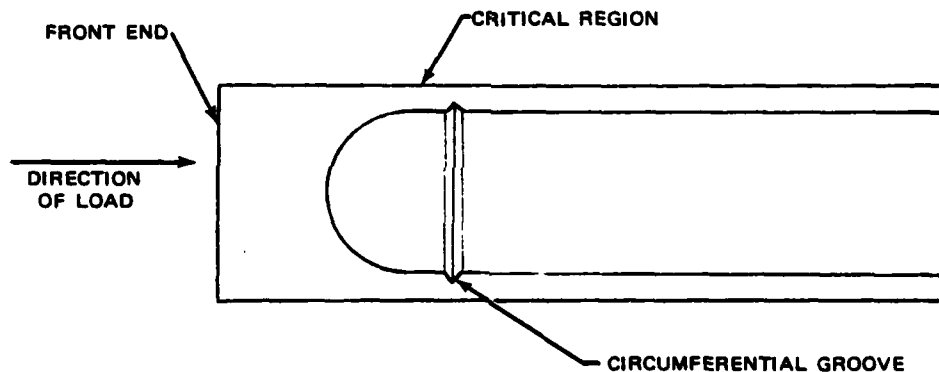


FIGURE 6. Circumferential Groove Replacing Complete Shear-Control Grid System for Purpose of Analysis.

The approach used was to study the effect of profile configuration, location, and depth on the stress and deformation patterns in a warhead case subjected to various impact loads for comparison with the response of a plain-walled case subjected to the same loads. The loads used were chosen to represent impact of moderately hard targets.

ASSUMPTIONS

This study assumed that the failure of the case depends on the magnitude and duration of the stresses experienced by sections of the case. Since the steels appropriate for a shear-control grid are ductile in order to achieve fragment control by shear, it is reasonable to expect

that the case will fail in a shear mode. (Full scale firings conducted under other programs have substantiated this mode of behavior.) A parameter widely used in the study of ductile failure is octahedral shear stress which is derived from the theory of maximum distortion energy. Octahedral shear is defined as

$$\tau_{\text{oct}} = 1/3\sqrt{(\sigma_2 - \sigma_1)^2 + (\sigma_1 - \sigma_3)^2 + (\sigma_3 - \sigma_2)^2} \quad (1)$$

where $\sigma_1, \sigma_2, \sigma_3$ are the principal stresses.

The octahedral shear stress at yield is

$$\tau_{\text{oct}} = \frac{\sqrt{2}}{3} \sigma_y \quad (2)$$

where σ_y is the uniaxial yield stress.

It was assumed that conclusions as to the effect of grid grooves on the failure of the case could be made by examining the octahedral shear patterns and structural deformations as predicted by the finite element code.

METHOD OF ANALYSIS

WARHEAD MODELS

Two finite element models were constructed for simulation using HONDO II, one with a circumferential groove and one without. Figure 7 shows the dimensions and the mesh construction.

The physical properties used for the 4340 steel are

density, ρ000733 lb sec ² /in ⁴
Poisson's ratio, ν3
plastic modulus, E_p	77,000 psi
yield stress, σ_y	148,000 psi

The two models were run against a pressure-time curve chosen to simulate penetration and perforation by the warhead of a 0.5-inch-thick mild steel target at 2000 feet/s. The resulting stress patterns were quite similar (Figure 8), with the stresses in the grooved warhead being only slightly higher and more persistent. It was found, however, that the similarity in response of the two models was due to the coarseness of the finite element mesh used, and that the finite element mesh would have to be much finer in order to reveal the effects of the groove with sufficient clarity to have any predictive value. Since a full-sized

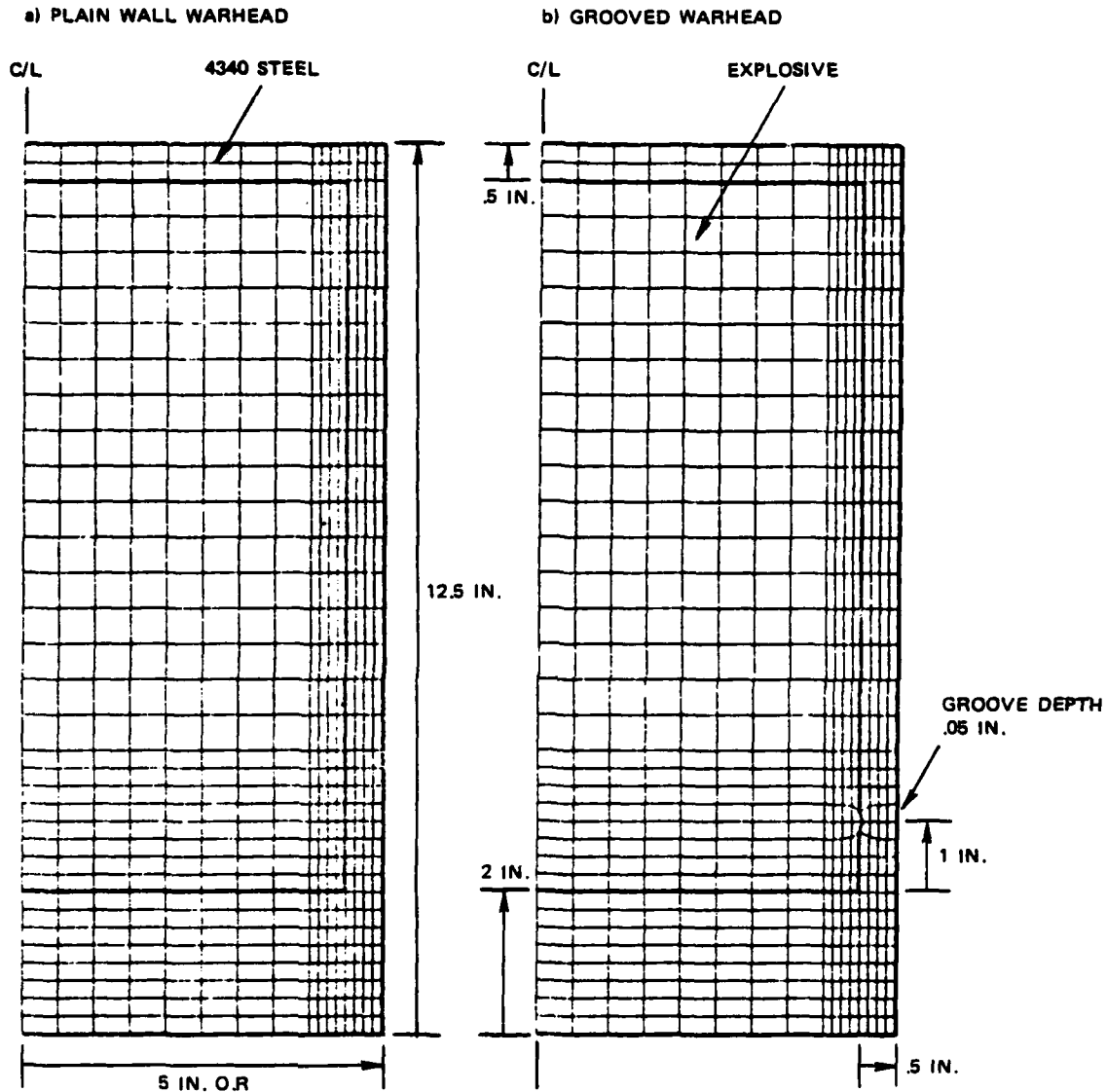


FIGURE 7. Finite Element Models of Warhead With and Without Circumferential Groove.

model with a sufficiently fine mesh would exceed the space allocated by the computer for HONDO II, it was necessary to study instead segments of the warhead case, thus allowing for meshes of sufficient resolution. The "full-sized" simulations provided information used to estimate the loads experienced by the case at the front plate interface. Simulation of the penetration into semi-infinite concrete using the full-sized warheads was not run as the information generated would not be cost efficient.

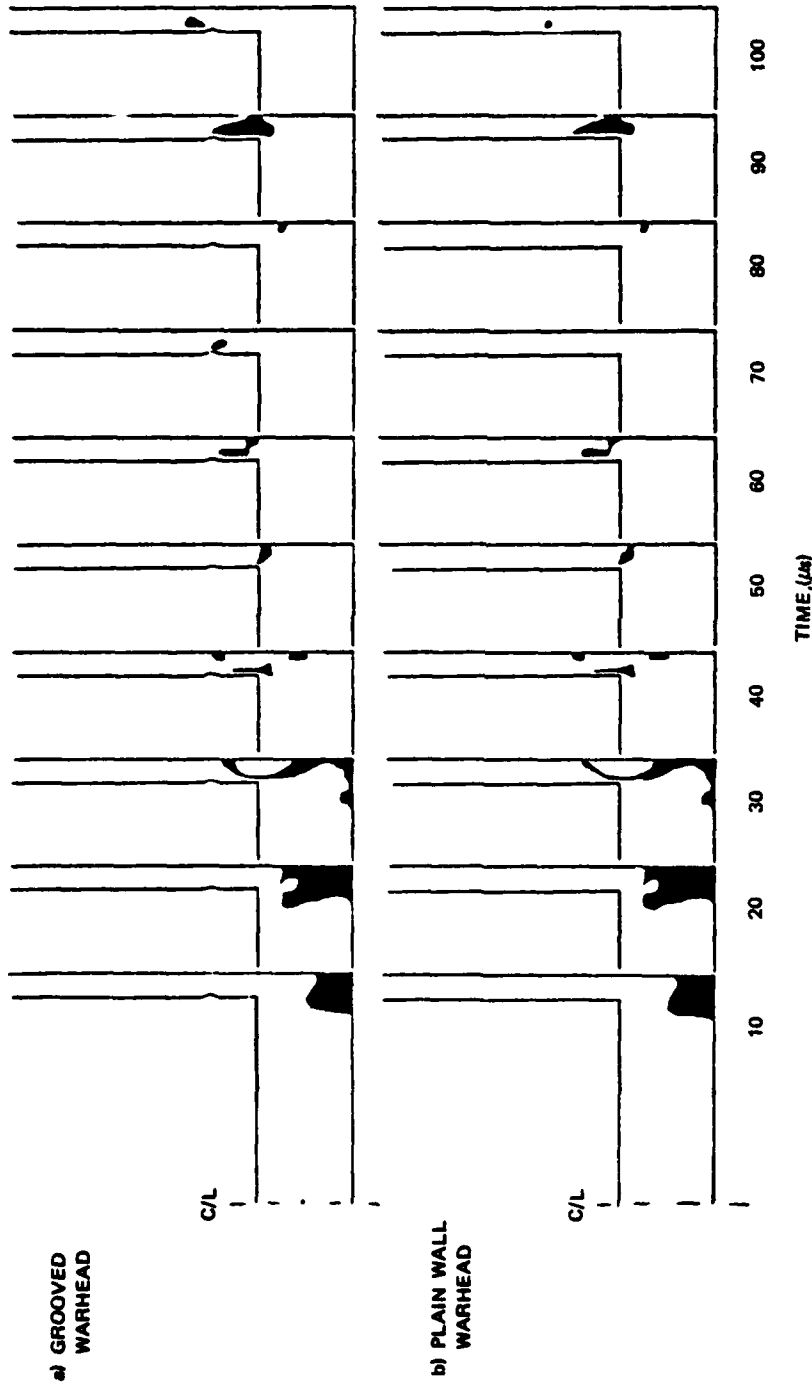


FIGURE 8. Regions of Yielding for Grooved and Plain-Wall Warheads Impacting a Steel Plate.

CASE SEGMENT MODELS

In order to study the effects of the grooves on the stress patterns in the warhead case with greater detail and generality, and at the same time keep the amount of computer time and cost within reason, finite element models of sections of the case were constructed. The loads placed on the case segments were similar to those experienced by case segments in the simulation involving the entire warhead. The finite element code was used to look at the effect of groove configuration, location, and depth on the stress patterns resulting from these loadings. The stress patterns generated in the case segments are predictive of the stress patterns that would be seen by sections of a case wall for an impacting warhead and thus, depending on the failure criterion of the case material, predictive of the failure of the warhead.

RESULTS OF THE CASE SEGMENT ANALYSIS

GROOVE CONFIGURATION

Figure 9 shows the structure mesh for the grooved and plain-wall case segments. Two groove orientations were used, as shown. The orientation of the groove is important to fragment control as the effectiveness of the nonsymmetric groove in producing primary shear trajectories is dependent on its orientation relative to the detonation wave. Figure 10 shows the three pressure-time curves used throughout this study. Curve A is the load derived from the full-sized study for perforation of a steel plate; curve B has a higher total impulse at the same pressure level; curve C has an extended, but less than yielding, load as would be experienced by the case during penetration of moderately hard targets (such as concrete). The actual load experienced by a case segment would depend on the impact situation. Here the loads are treated as an independent parameter.

The load given by curve A of Figure 10 was applied to the segment end of each of the three configurations. Figures 11(a) and 11(b) show the octahedral stress contours (10,000, 40,000, 70,000 psi) for the plain-wall and grooved case segments, with the regions of yielding blackened in. Two stress waves move the length of the segment past the groove position and into the shock absorber portion of the test specimen--an elastic wave and a slower moving plastic wave. The plastic wave dissipates and the plastic portion reaches a maximum distance of 0.6 inch into the segment and then vanishes as the load is removed. There is no other plastic region in the plain-wall specimen. In contrast, the grooved segments show (and this proved to be characteristic) two bands of yielding emanating from the groove position and running at 45 degrees to the compressive load, the direction of maximum shear. The stress patterns are clearly independent of the groove orientation, as shown by Figure 12, and the planular regions

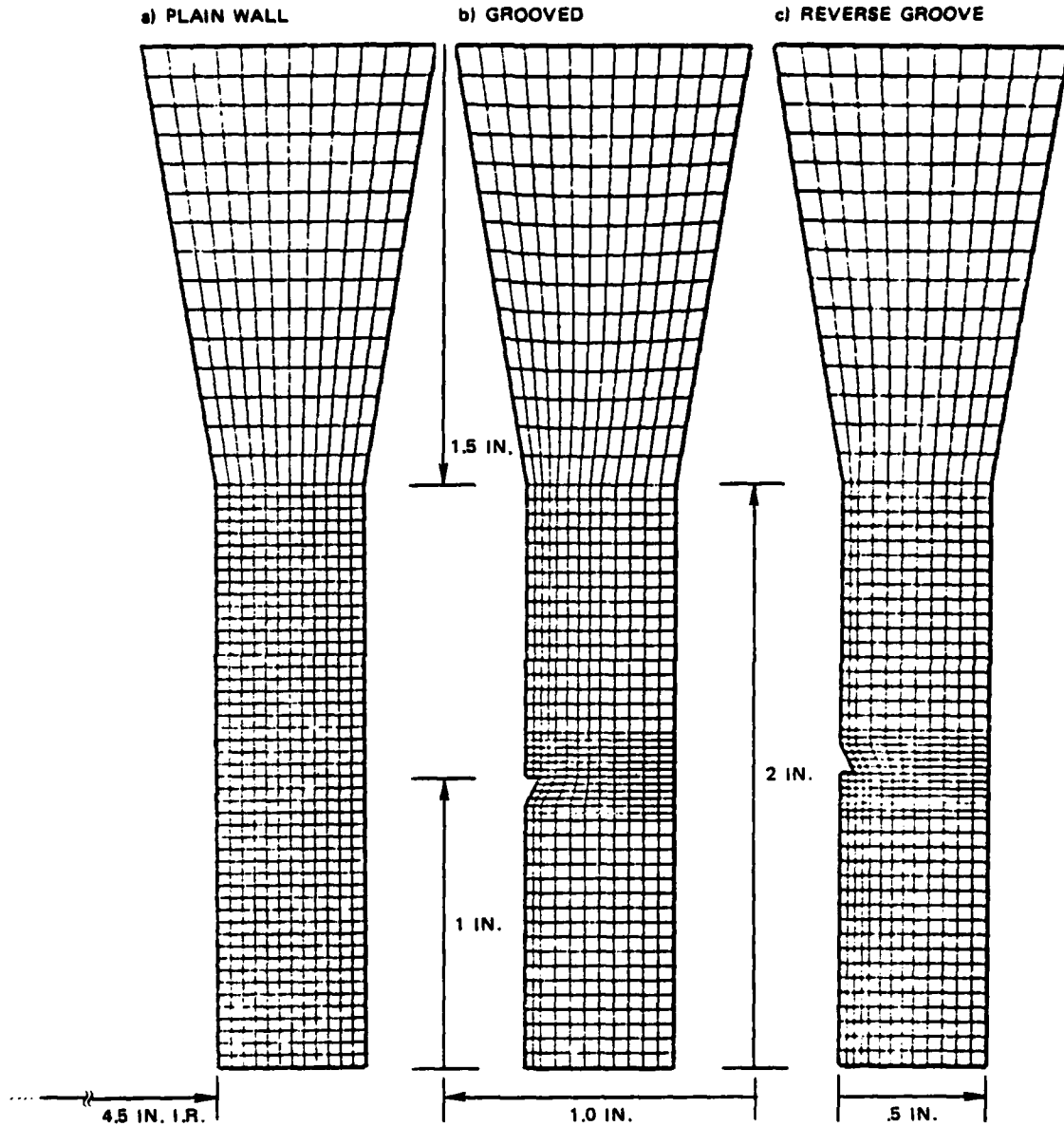


FIGURE 9. Finite Element Model of Grooved and Plain-Wall Case Segments. Notch depth, .05 inch; notch width, .1 inch.

of yielding are certainly a result of the presence of the groove. In this example, the bands of yielding extend the width of the case and last for approximately 13 microseconds. A failure criterion for the case would depend on the length of the yielding band, particularly on whether it spans

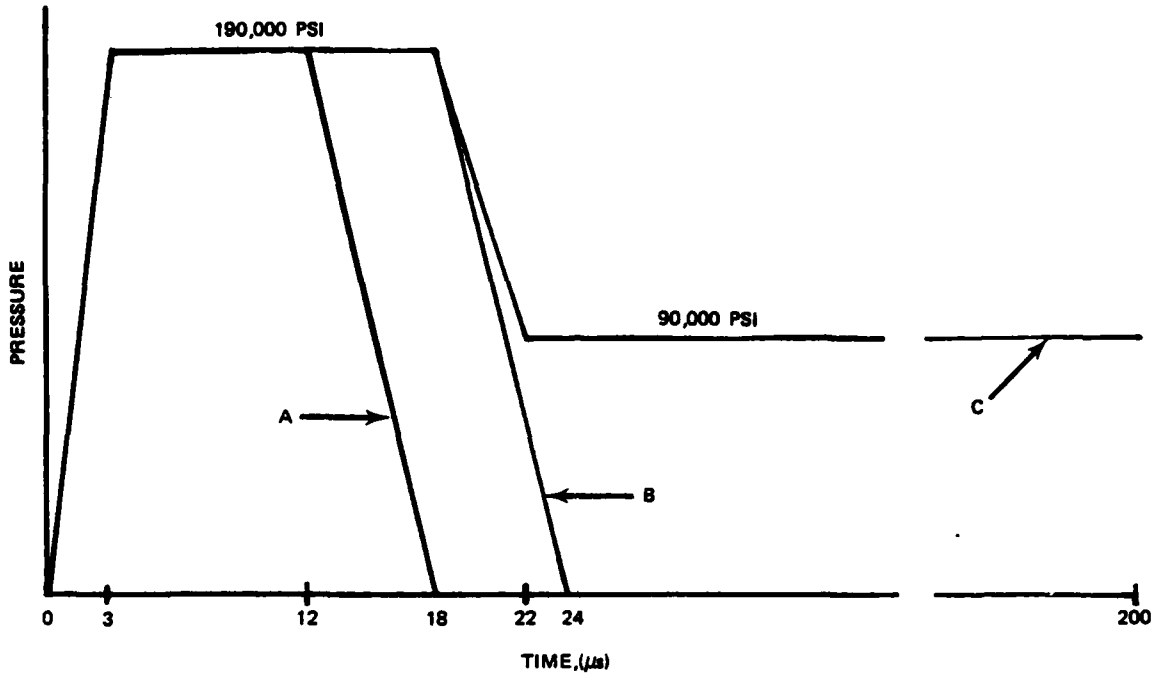


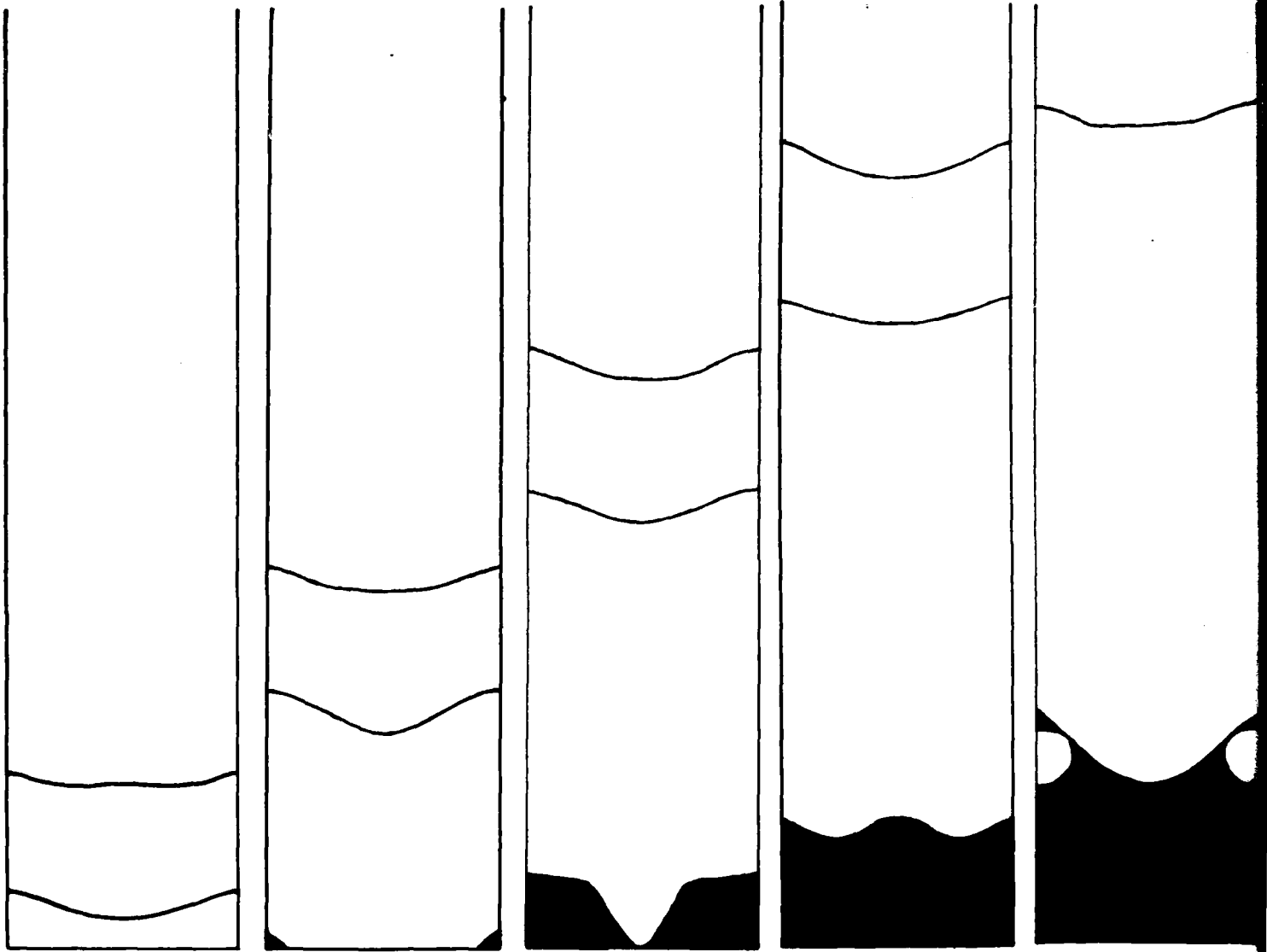
FIGURE 10. Pressure Versus Time Curves Applied to Test Specimens of Case Segments.

the case width, and on the duration of the span. A successful failure model would have to be predictive of the type of failure (either ductile or brittle) in order to estimate the time at which the case failed.

While the shape of the groove is fairly well set by the application, it can be expected that any triangular-shaped groove that has about the same depth as those investigated here will generate basically the same stress pattern consisting of the 45-degree bands of yielding originating at the groove position. Thus, it is expected that similar failure patterns will result even from different groove profiles.

GROOVE LOCATION

The case segments tested for the effects of groove configuration were located in what would be the weakest portion of the full warhead, that is, near a region experiencing the maximum stresses and showing the greatest deformation. One possible way to avoid the detrimental effects of a shear-control grid would be to keep it behind the region of the case/front plate interface. Figure 13 shows mesh structures for nonsymmetrical and "vee" grooved case segments, with the distance between the segment end and the groove position extended from 1 to 2.5 inches. Load A of Figure



2

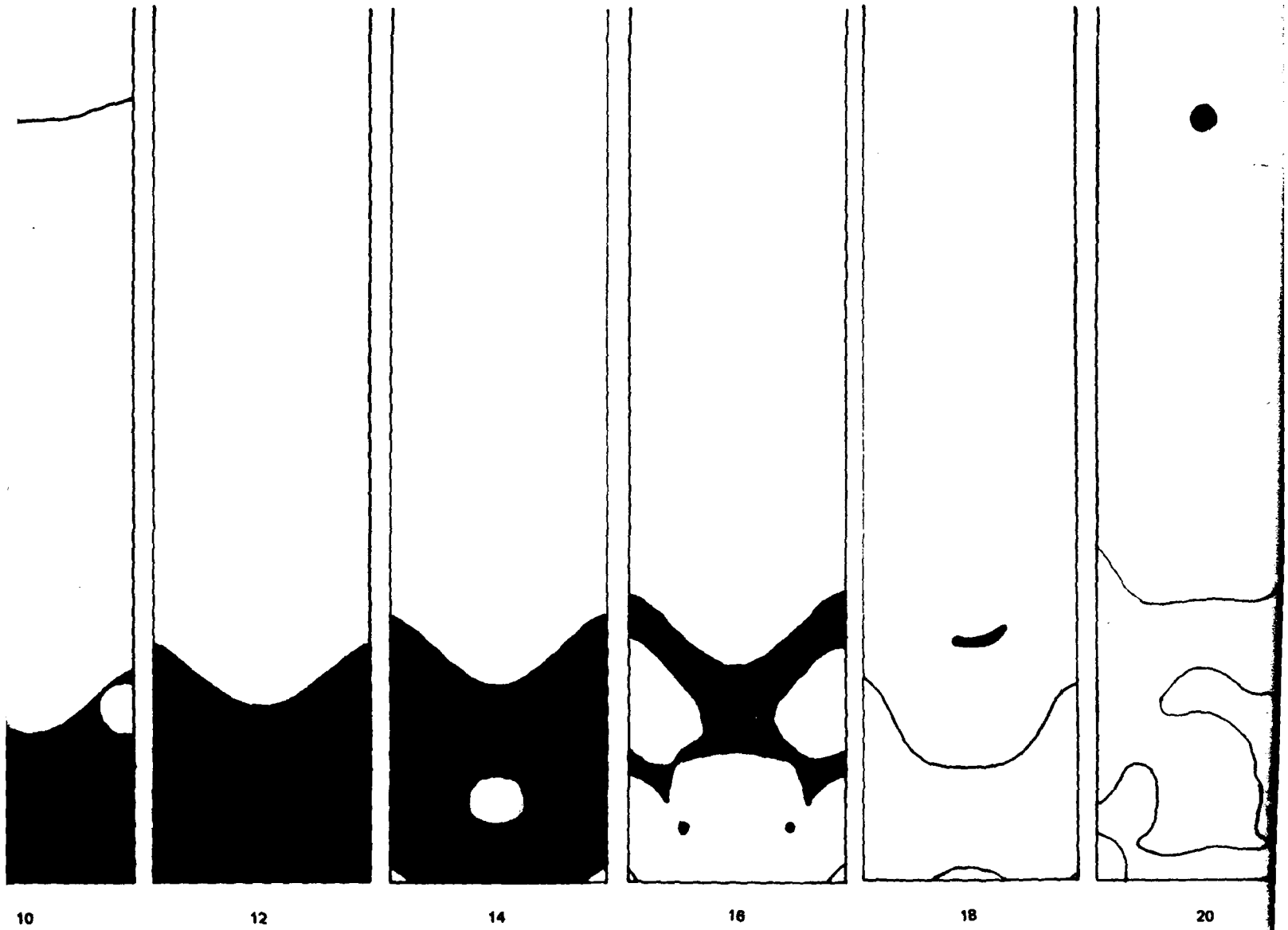
4

6

8

10

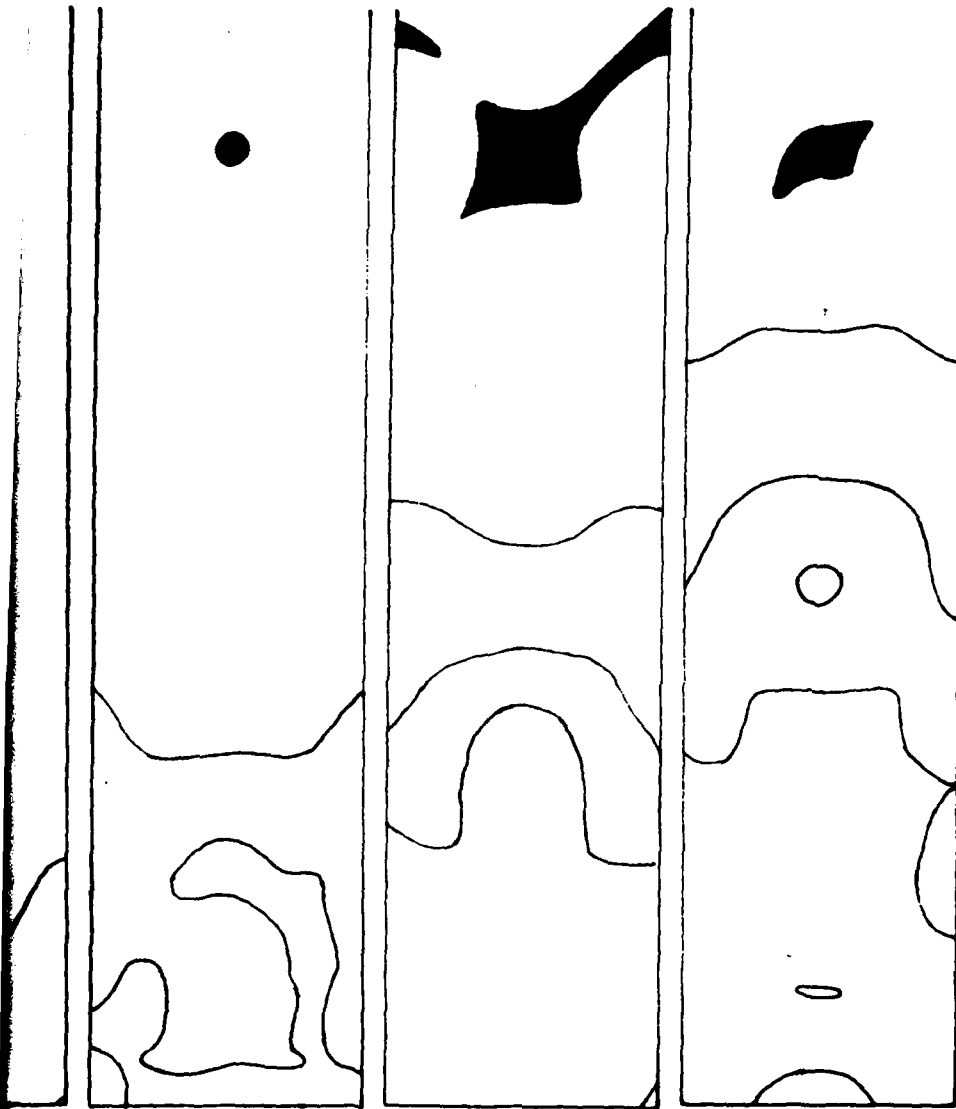
TIME, (μ s)



(a) Plain-Wall Cylinder
FIGURE 11. Regions of Yielding.

12

NWC TP 6288



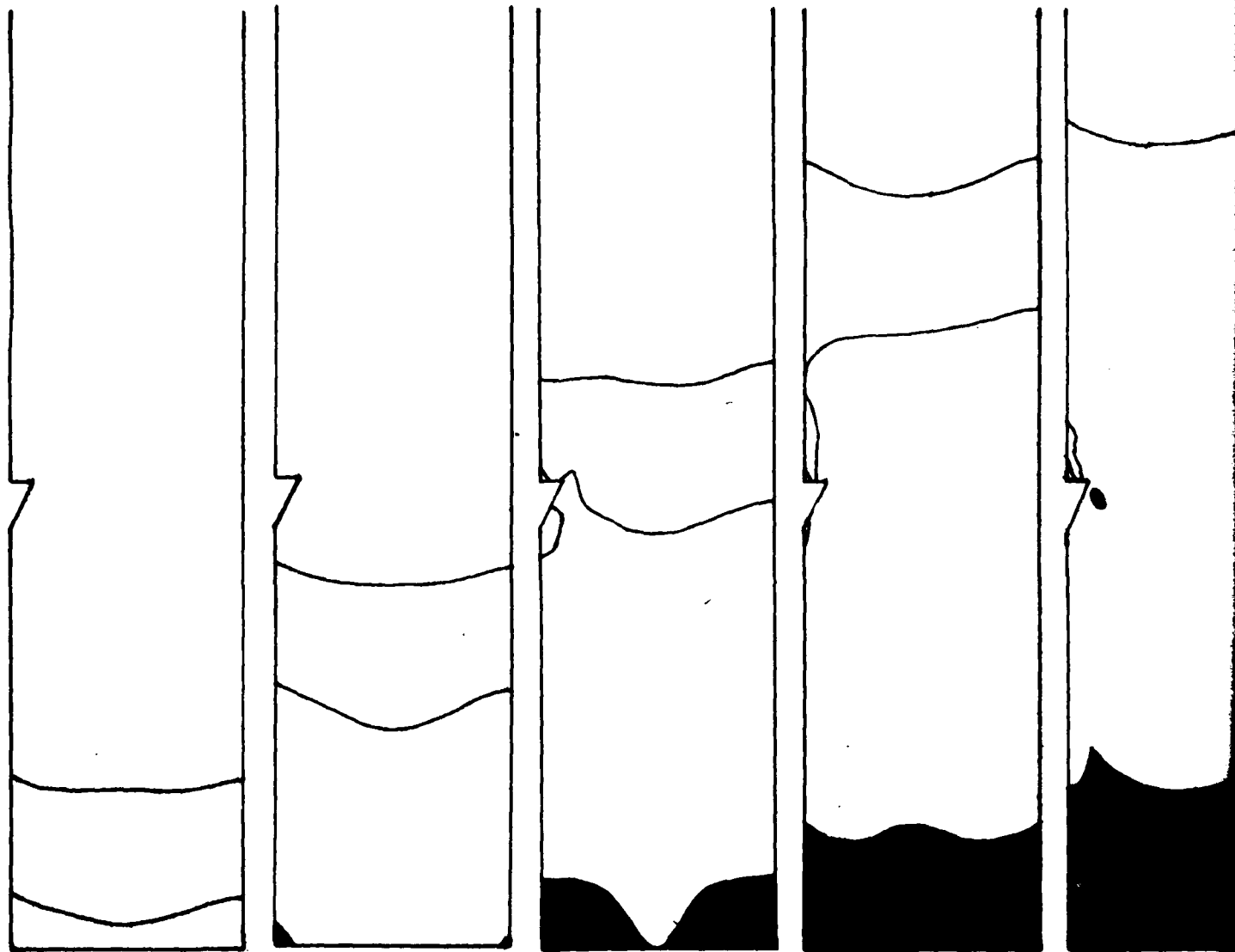
20

22

24

17/18

1 13



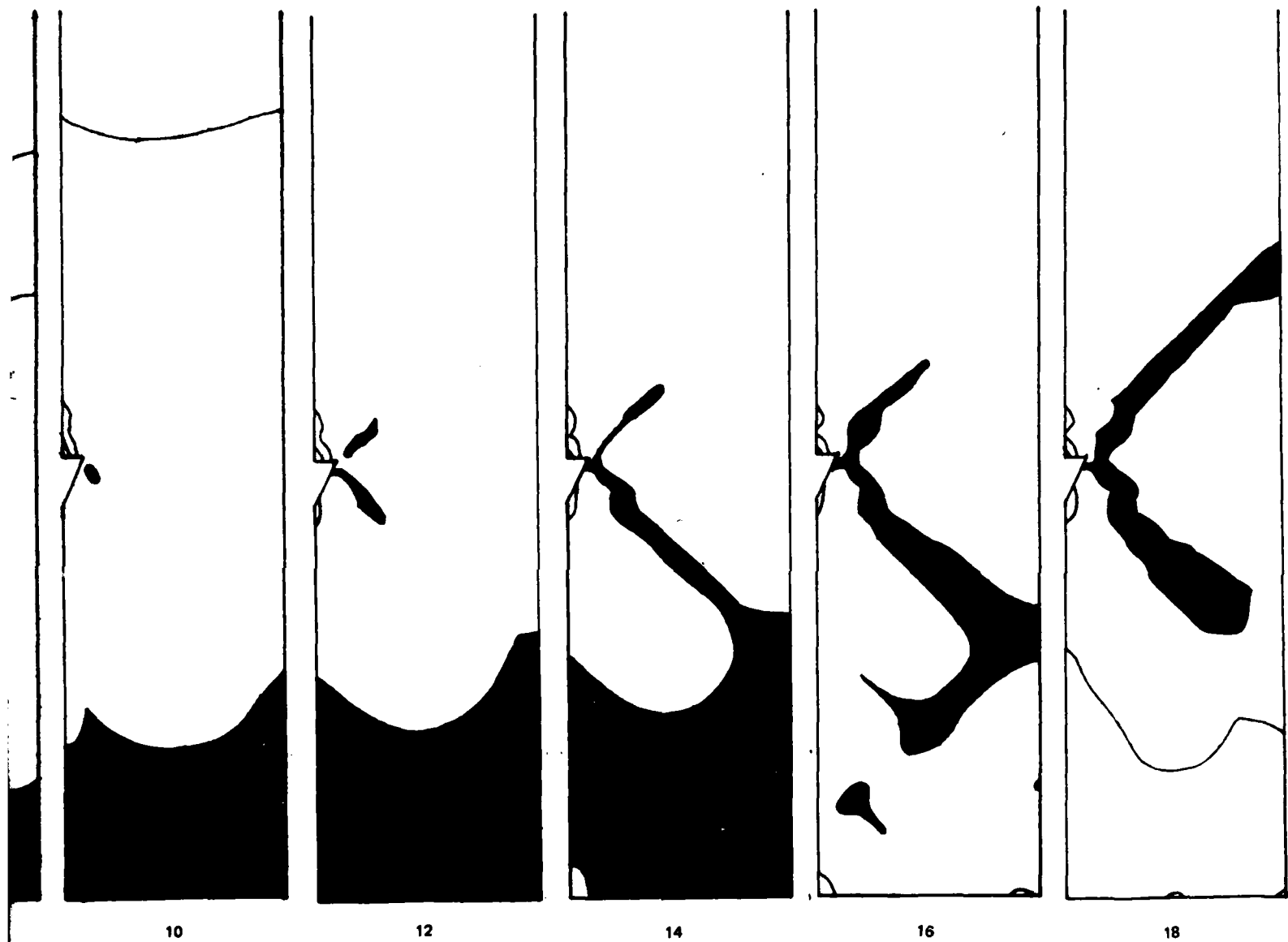
2
TIME, (μs)

4

6

8

10

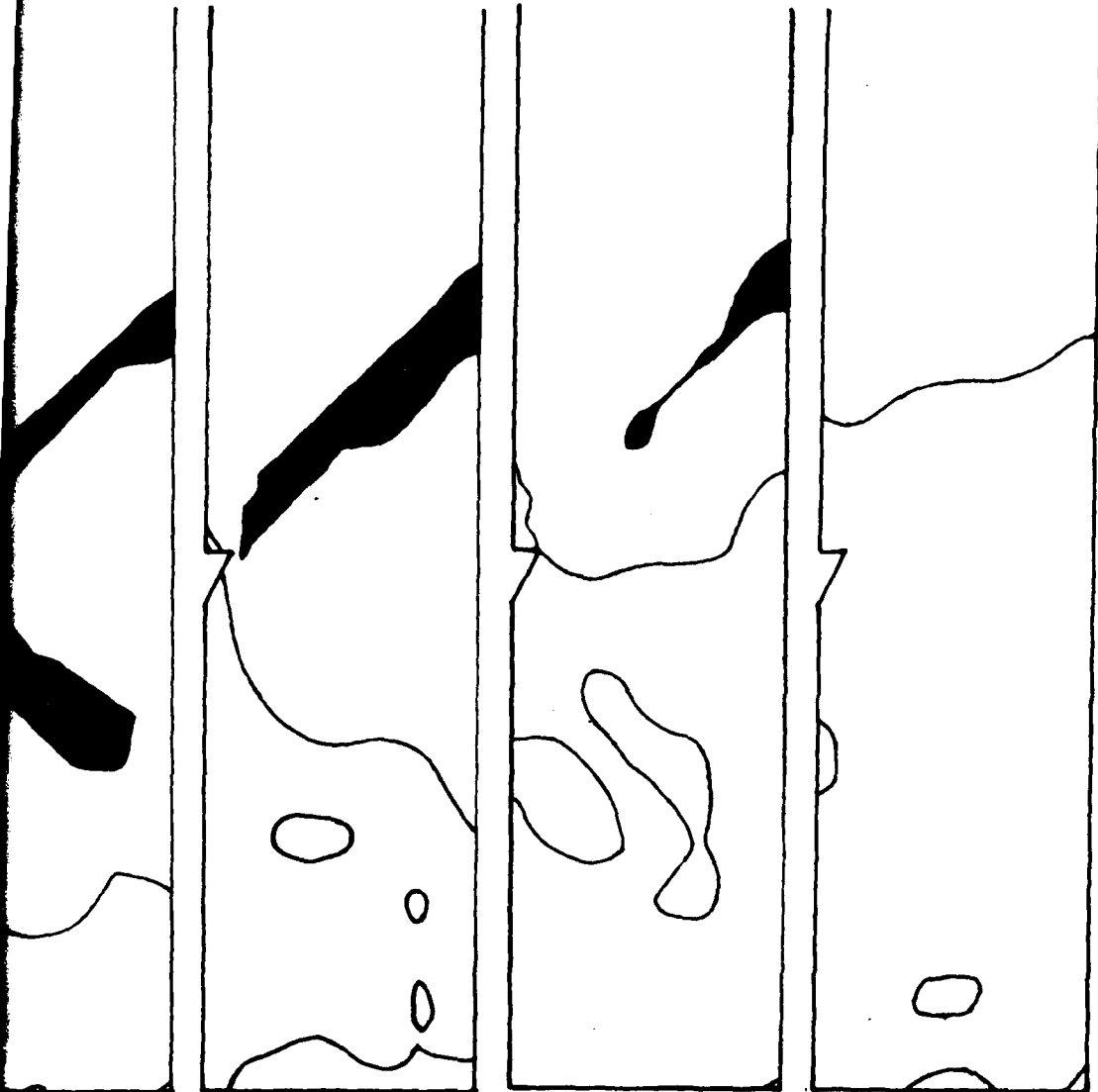


(b) Grooved Cylinder.

FIGURE 11. Regions of Yielding.

12

NWC TP 6288



18

20

22

24

19/20

3

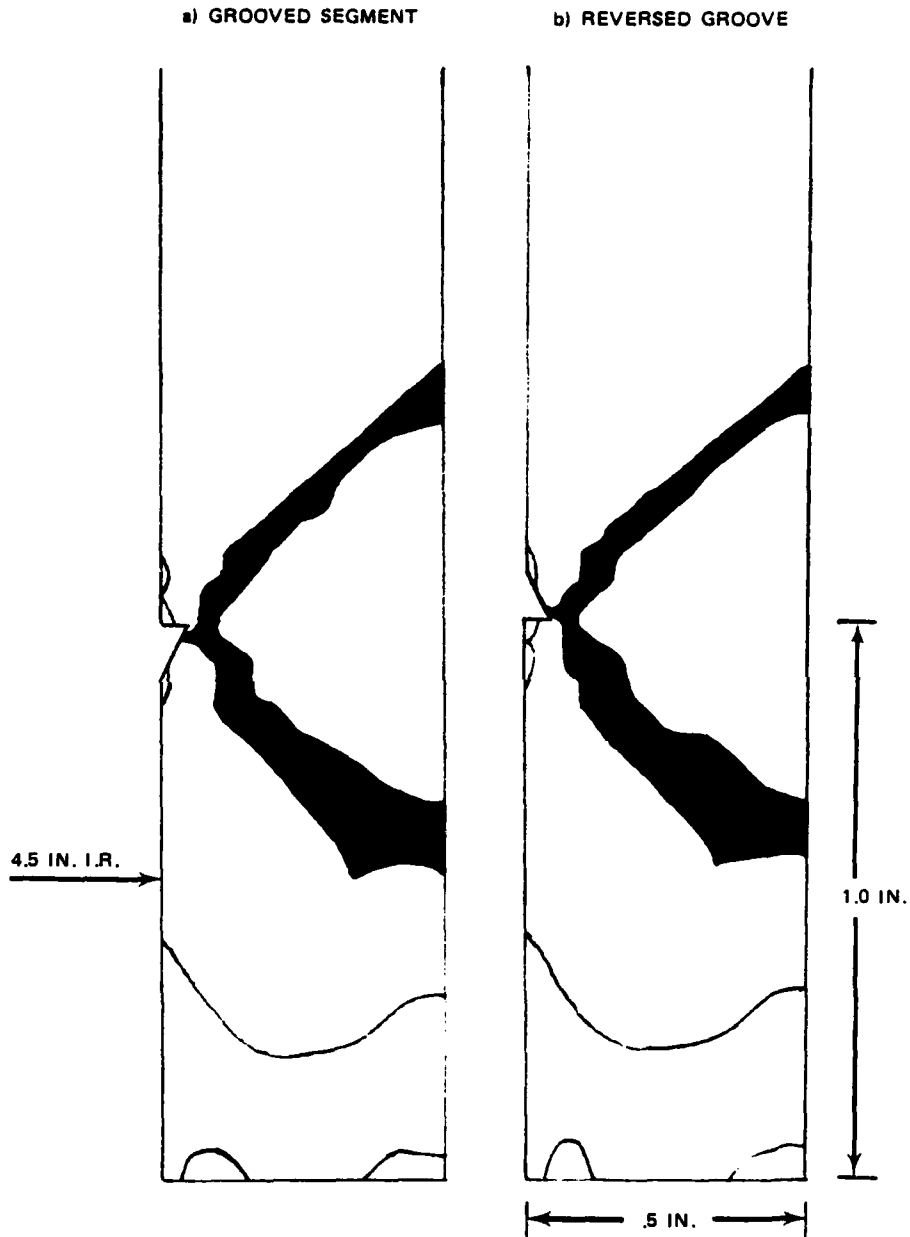


FIGURE 12. Regions of Yielding for Grooved Case Segments of Two Orientations at 17.5 Microseconds After Application of Load Given by Curve A of Figure 10.

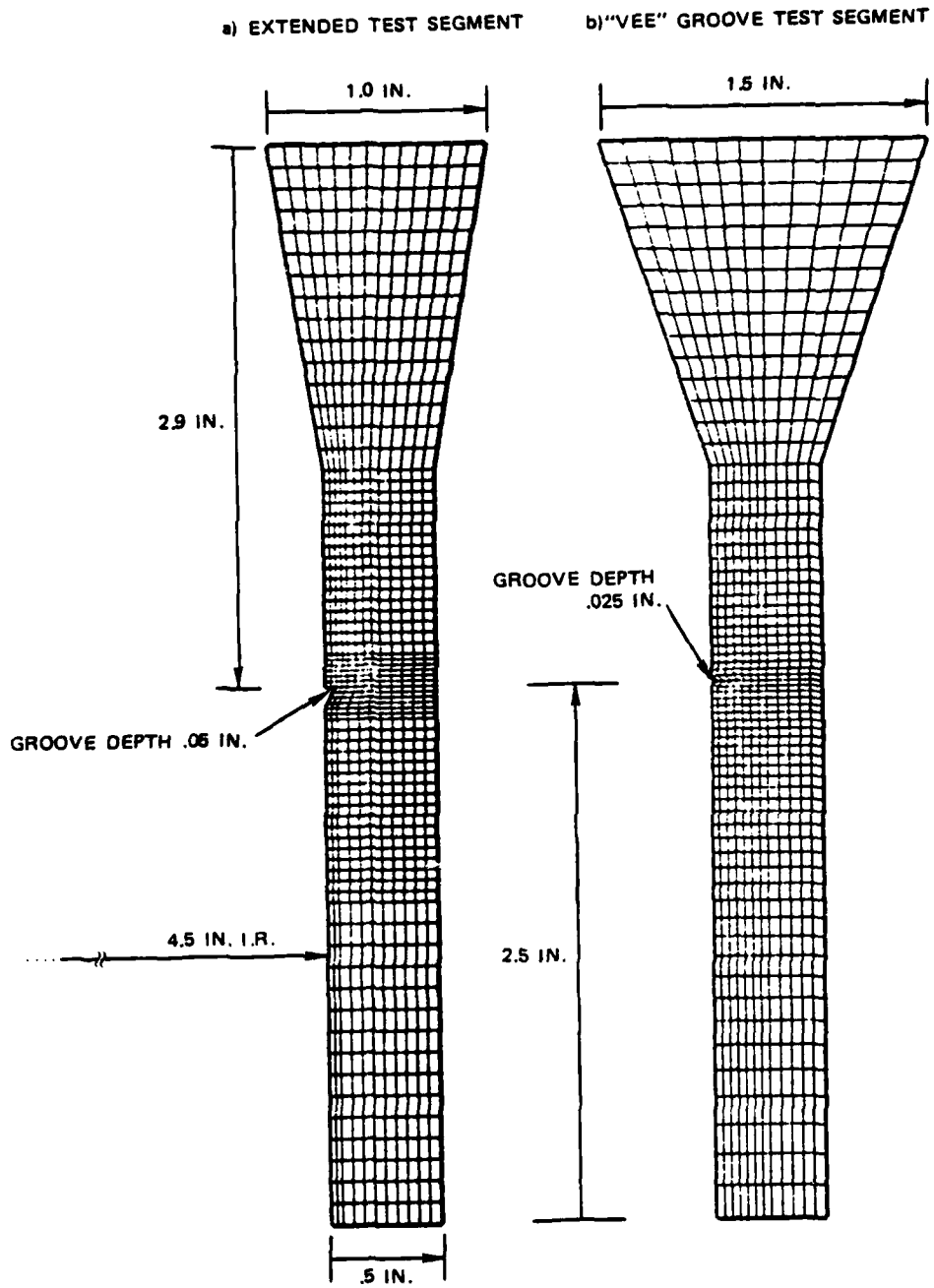


FIGURE 13. Finite Element Models for Extended Test Case Segments With Nonsymmetric and "Vee" Groove.

10 was again applied to the extended test specimen shown in Figure 13(a). The stress patterns generated are shown in Figure 14. Linear regions of yielding again appear at the groove, but extend only partially through the width of the case, and have a duration of 10 microseconds, 3 microseconds less than the duration of the yielding zones for the groove placed nearer the segment end. Thus, the likelihood of case failure can be reduced by moving the initial groove farther from the region of greatest stress. (The apparent offset of the yielding zone from the root of the groove is due to limits imposed on the contour plotting routine by the size of the elements in the finite element mesh at the groove root.)

EXTENDED SEGMENT

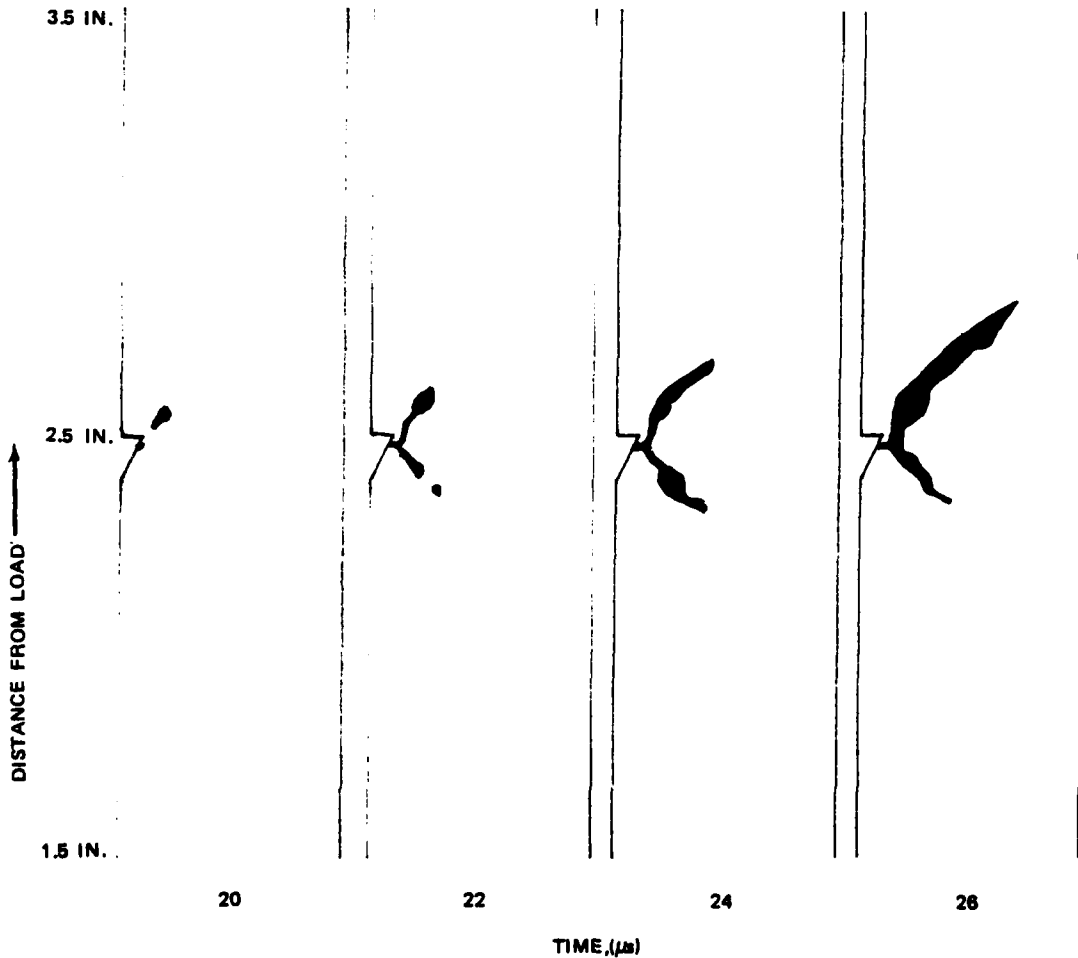


FIGURE 14. Regions of Yielding for Extended Test Case Segments Showing Maximum Extensions of Region at 26 Microseconds.

The results of applying the load of greater duration (curve B of Figure 10) to the lengthened specimen are shown in Figure 15. Until 26 microseconds the stress contours exactly duplicate those shown in Figure 14. In the previous test the linear zones begin to recede at this time. In this test the zones continue to lengthen and finally span the width of the case. The region of yielding at the front of the specimen extends a maximum of 0.8 inch along the length of the case, an increase of 0.2 inch. The duration of the yielding bands for this test was 18 microseconds. It

EXTENDED SEGMENT, LONGER LOAD

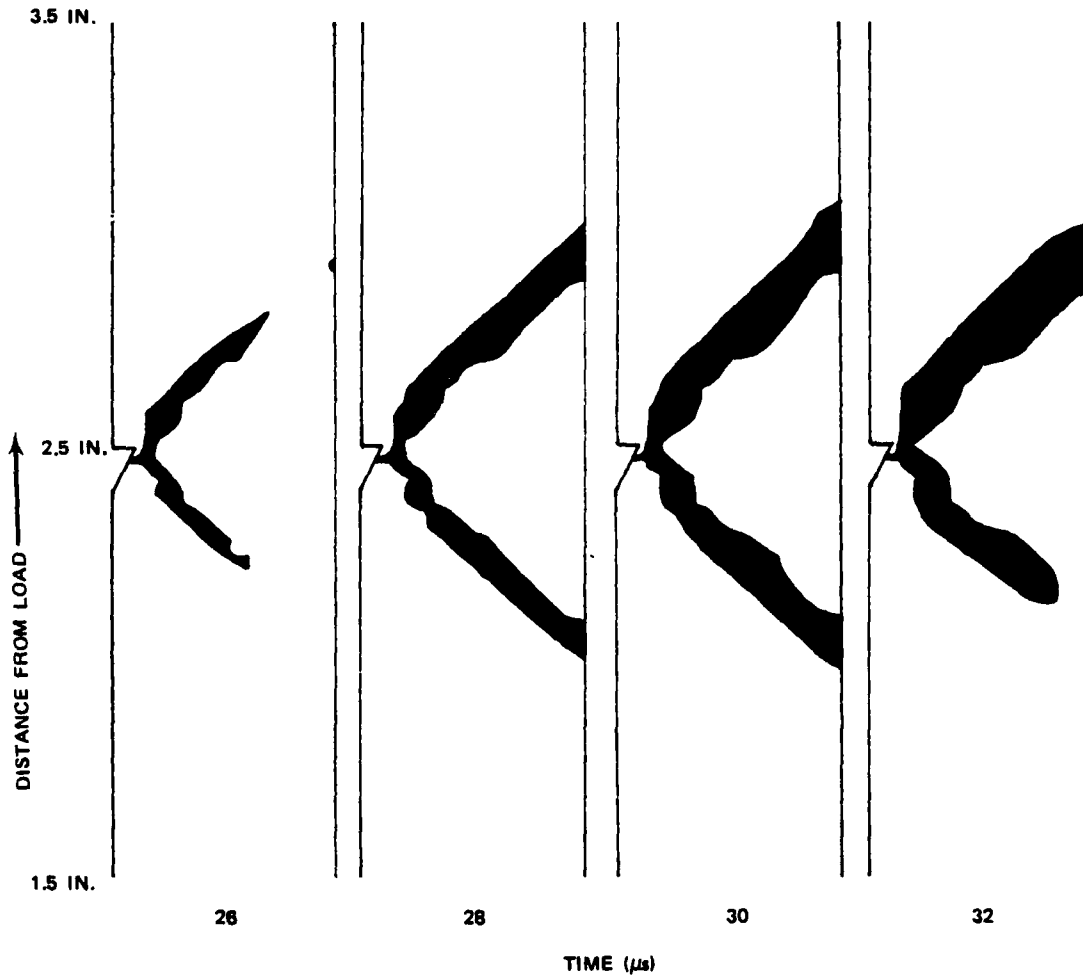


FIGURE 15. Regions of Yielding for Extended Test Case Segment Under Longer Load Duration Showing Maximum Extension at 30 Microseconds.

is evident that the extent and duration of the linear zones of yielding depend on the distance of the groove from the region of greatest stress and on the duration of the load. Thus, the probability of warhead failure increases as the duration of the load increases for warheads with and without grid systems.

DEPTH OF THE GROOVE

Besides moving the grid system away from the case loading points, another possible method of resisting failure due to the presence of a shear-control grid would be a reduction in groove depth or, alternatively, an increase in case thickness. Unfortunately, the nonsymmetrical groove profile that is used for precision fragmentation control requires a minimum depth of about 0.040 inch. However, the symmetrical "vee" groove, which is used for nonprecision control, can be effectively used with a depth of only several thousandths of an inch.

Figure 13(b) showed the finite element mesh for a case segment having the same dimensions as the extended segment used in the preceding study of groove location but having a shallow "vee" groove. This "vee" groove test segment was subjected to the same load (curve B of Figure 10), which caused bands of yielding to extend the width of the case with the presence of the larger nonsymmetric groove. Figure 16 shows the extent of the bands of yielding caused by the "vee" groove. Most of the yielding occurs upon the return of the stress wave from the far end of the test specimen, and little yielding is associated and none is actually connected with the "vee" groove. This shows that the failure of the case can be made less likely by a reduction of the groove depth. Some caution must be exercised in interpreting this last simulation. The mesh detail near the small groove was taken to be one element because of computer run-time considerations. Thus the material near the groove may react too stiffly, and the extent of the regions of yielding predicted by the finite element simulation may be too small. However, the basic conclusion that reduction in groove depth enhances the survivability of the case is reasonably certain.

That the relative depth of the groove is important in determining the survivability of the case is shown by the following test made to study the effect of increasing the wall thickness of a test specimen on the growth of the yielding regions caused by the groove. The width of the finite element model shown in Figure 13(a) was increased by 50%, resulting in the model shown in Figure 17. The structure was subjected to the load detailed by curve B of Figure 10. Figure 18 shows the region of yielding for the extra wide case segment. Comparing the contours for the normal and extra wide case segments, we see that the extent of the lower band of yielding is reduced and that the upper band does not span the width of the thicker case. Additionally, the duration of the yielding process in the groove region is reduced from 18 to 12 microseconds.

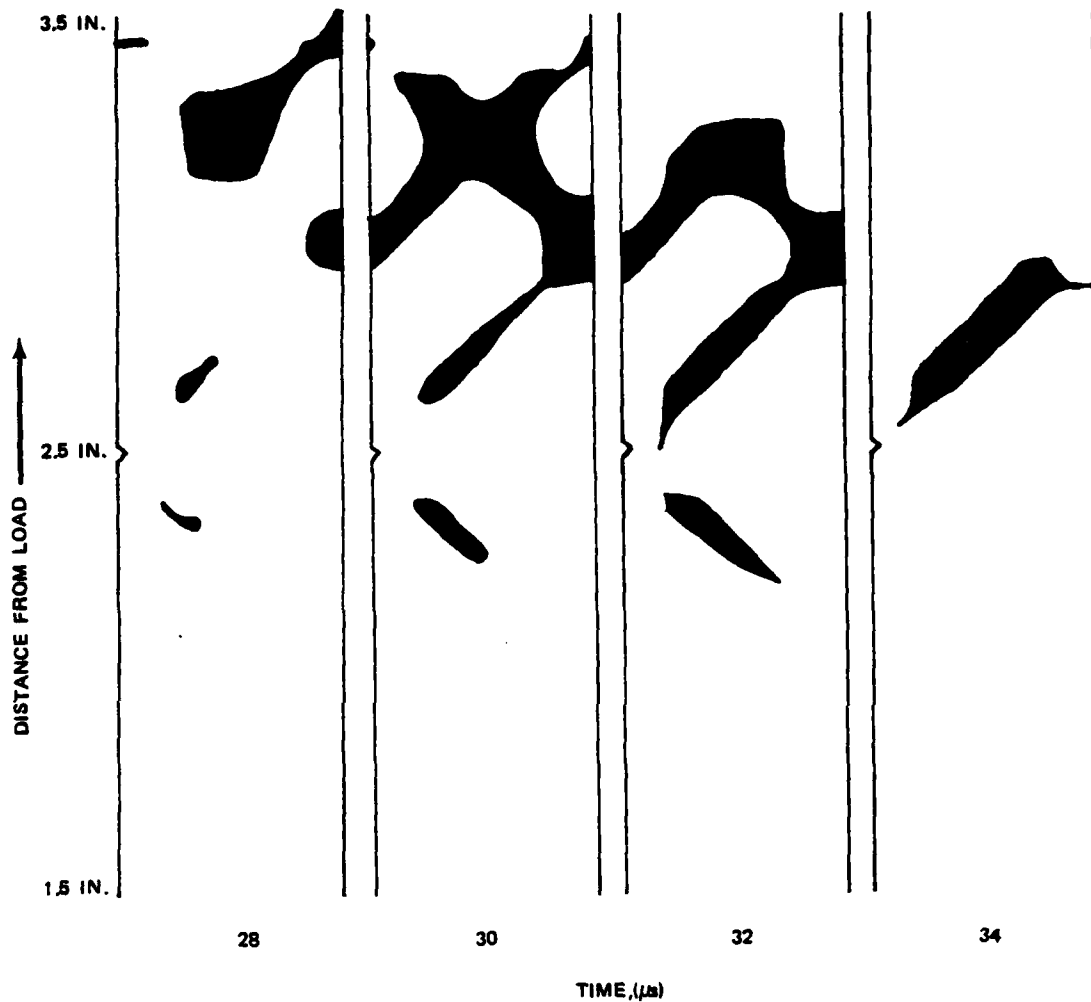


FIGURE 16. Zones of Yielding in Shallow "Vee" Grooved Segment Subjected to Load.

Thus the survivability of the case is enhanced by either a reduction in groove depth or by an increase in wall thickness. The depth of the groove relative to the case thickness is important in determining the survivability of the case.

GROWTH OF THE BANDS OF YIELDING

A summary of the effects of groove location, relative depth, and load duration on the growth of the notch yielding bands across the width of the case is given by Figure 19 for two different case thicknesses. For each test, the radial extent of the region of yielding appears to

NWC TP 6288

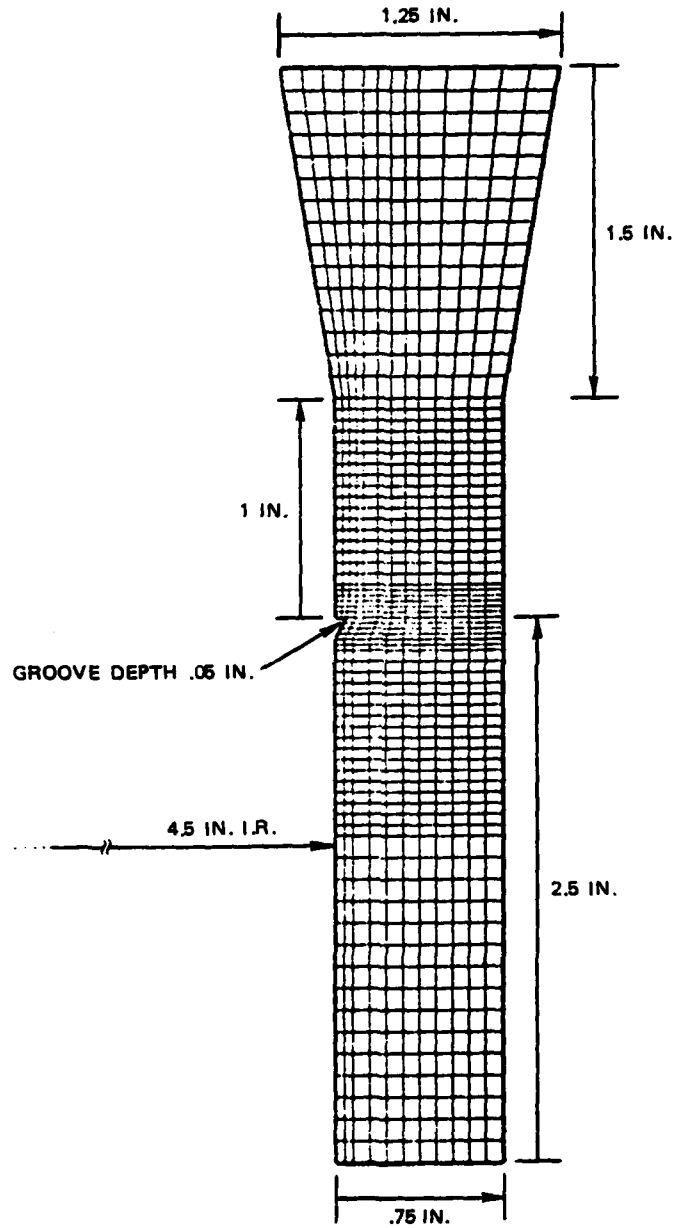


FIGURE 17. Finite Element Model of Case Segment With .75-inch Wall Thickness.

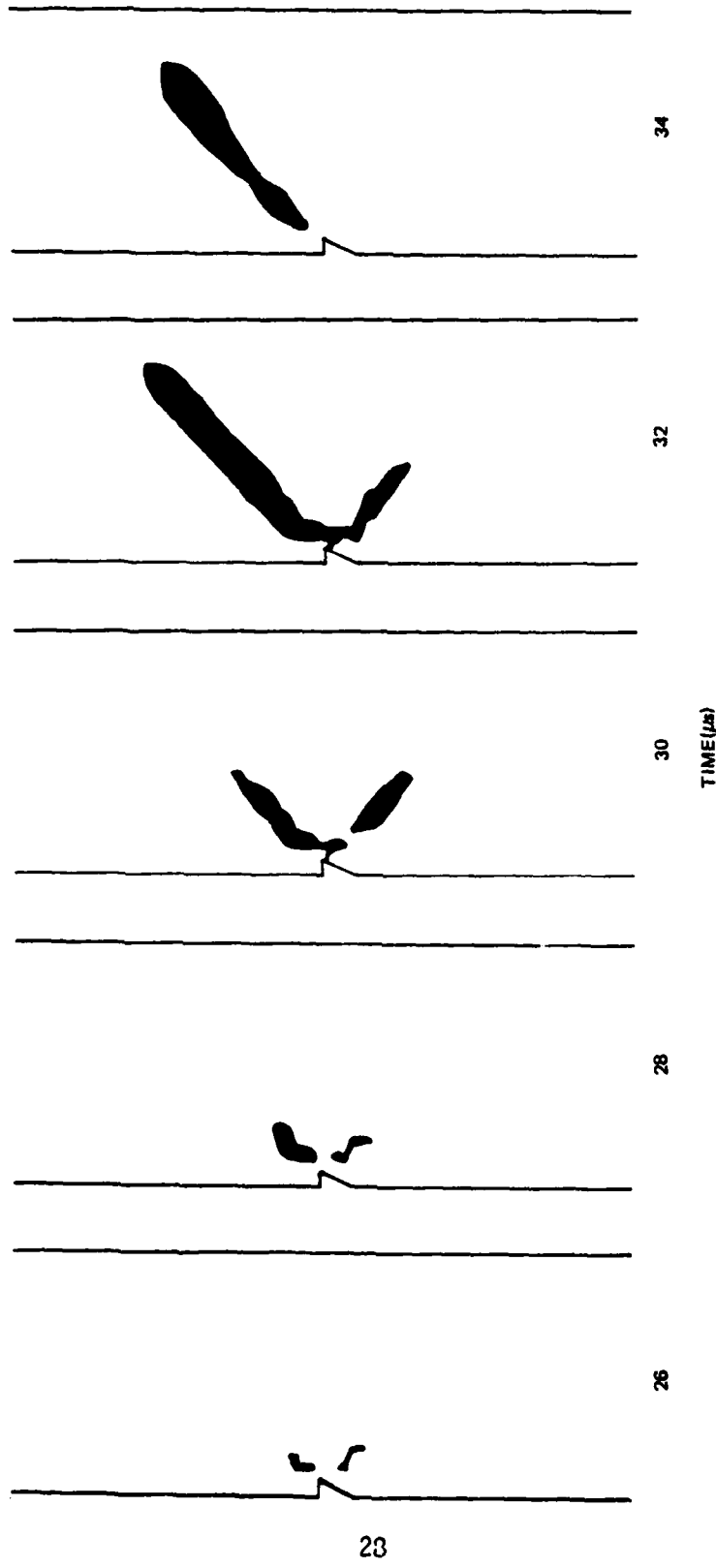


FIGURE 18. Regions of Yielding for Extra-Wide Case Segment.

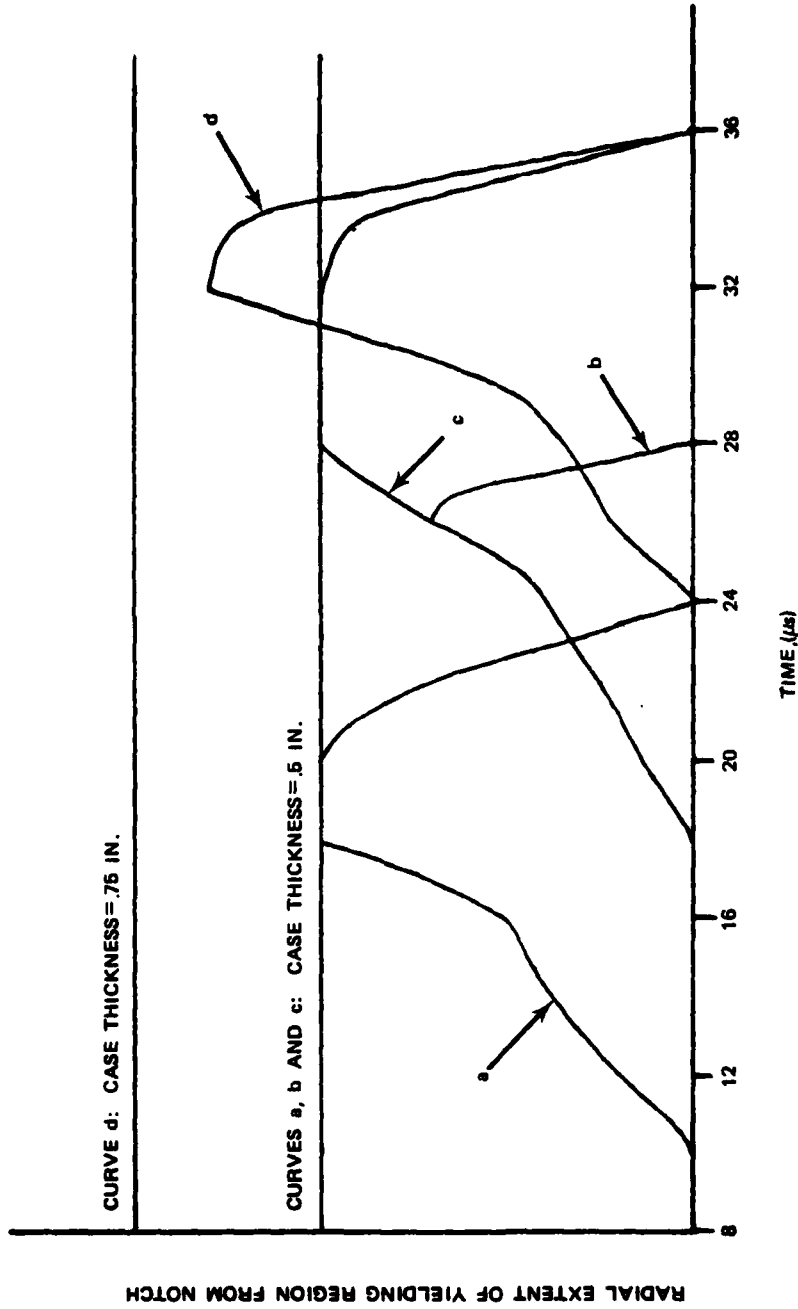


FIGURE 19. Extent of Radial Yielding Region From Notch. Notch distance from load 1 inch in curve a; 1.5 inch in curves b, c, and d. Pressure-time given by Curve A of Figure 10 for curves a and b; by Curve B of Figure 10 for curves c and d.

grow with time in a very roughly exponential manner until either the case width is spanned or the load on the specimen is removed. When the load is removed from the test specimen, the region of yielding retreats back to the groove. The growth rate for the extended segments (curves b, c, and d) is less than that for the segment with the groove nearer the load (curve a). For curve b, the band does not have time to span the case. Curve c shows the band of yielding spanning the case width for a load of the same magnitude but of greater duration. Thickening the case resulted in an initial delay in the initiation of the yielding (curve d), but once begun, the band length for the thicker case grew at a higher rate than did the bands in the thinner specimens.

CASE DEFORMATIONS

The deformations of the case segments from which the stress contours were obtained were small. This is because the run times were relatively short in comparison to run times usually used for full warhead simulations. Finite element structures of grooved and plain-wall case segments were constructed for the purpose of examining the deformations resulting from application of loads of long duration on the two types of segments. The mesh was made less detailed near the groove to compensate for the longer run times, and so may have reacted somewhat more stiffly to the stresses, producing smaller deflections and more diffused dislocation patterns.

The pressure-time curve applied to the segment end is shown by curve C of Figure 10. After 150 microseconds the plain-wall case segment shows no great deformation at its midsection, and is, in fact, locally concaved (Figure 20). Gross deformations are concentrated at the ends. In contrast, the grooved segment shows a clear pattern of relatively large deformation (Figure 21). The midsection deformation is largely confined along the lines of yielding seen in the previous runs, and maximum displacements appear along lines extending from the groove at 45 degrees. A torus with a triangular cross section is being pushed outward from the wall of the case. The groove is forced closed. By this time in the simulation it is apparent that the grooved case is more likely to satisfy some failure criterion than is the plain-wall case, and at least a well defined circumferential ring appears on the outside surface of the grooved case and not on the plain-wall case.

The deformation pattern, which might be called the groove ring, is caused by the bands of dynamic yielding that are associated with the groove and to which the plastic flow in the area of the groove is constrained, and by the moment created by the offset of the compressive load due to the presence of the groove, which allows plastic strain in directions along the length of the bands. For a full grid system, providing that the case does not fail, one may be able to see the outline of the grid on the outside of the case wall, provided the load is long enough, just as the outline of a shear-control grid can be seen in the initial

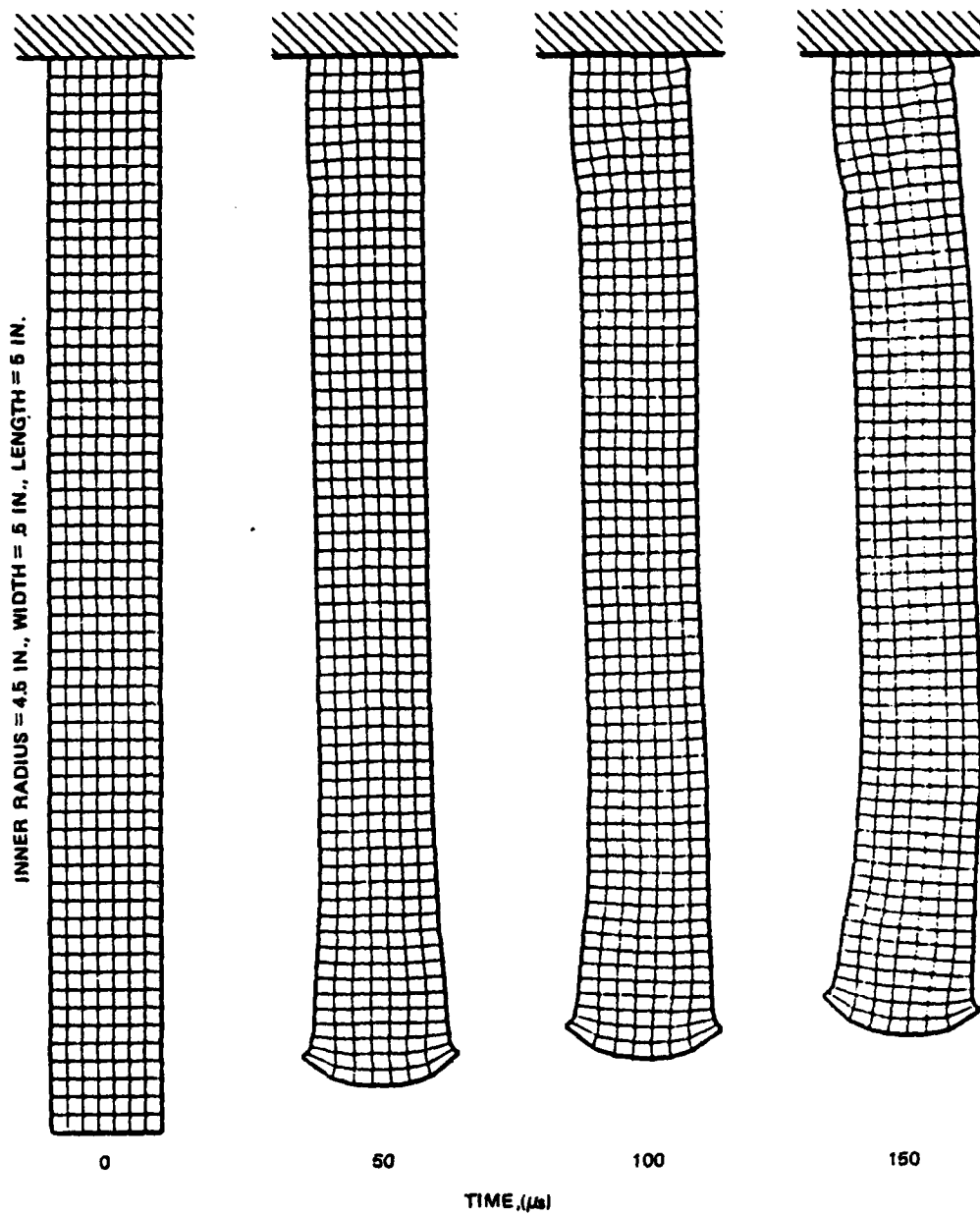


FIGURE 20. Plain-Wall Case Segment Deformation Resulting From Load C.

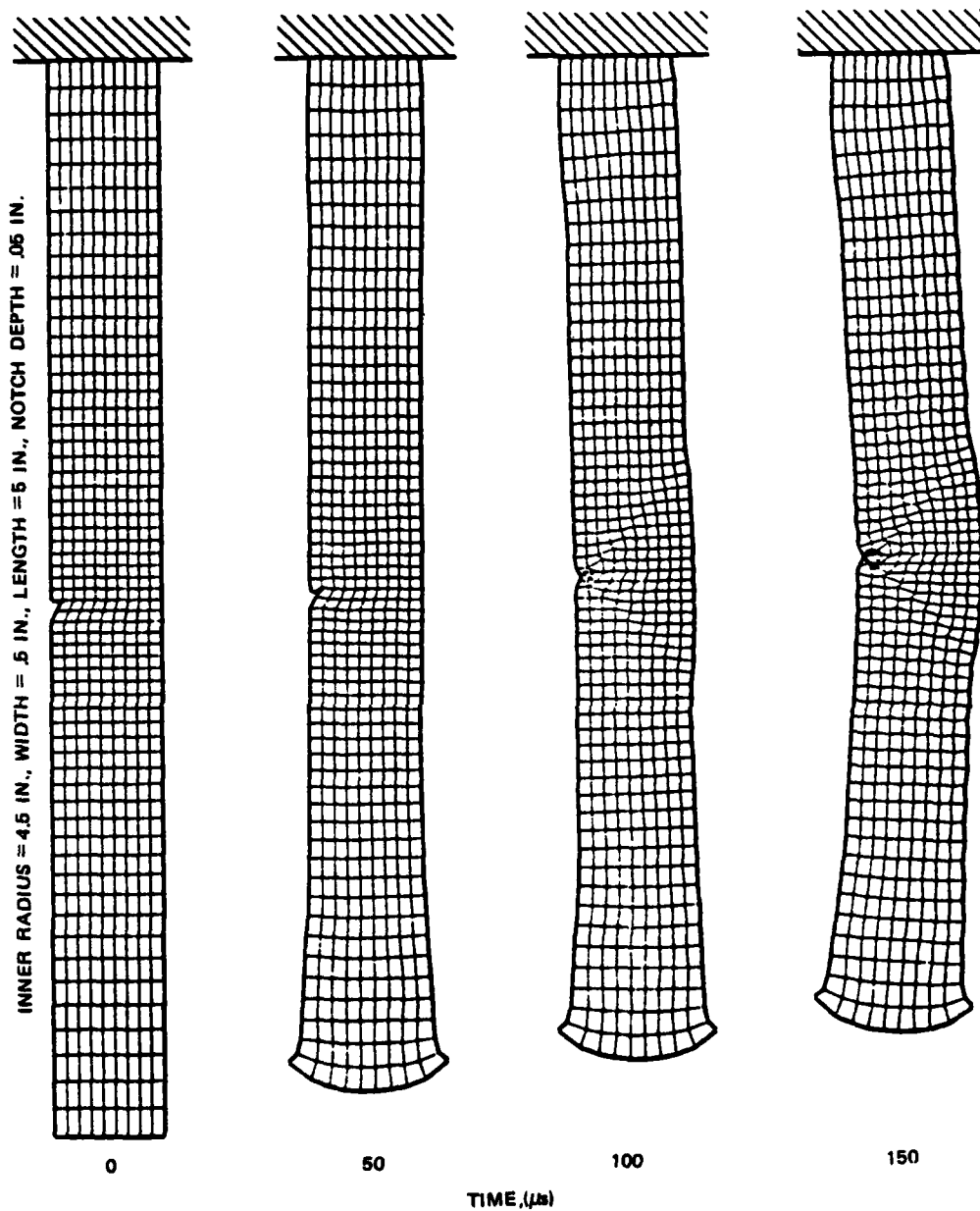


FIGURE 21. Grooved Case Segment Deformation Resulting From Load C.

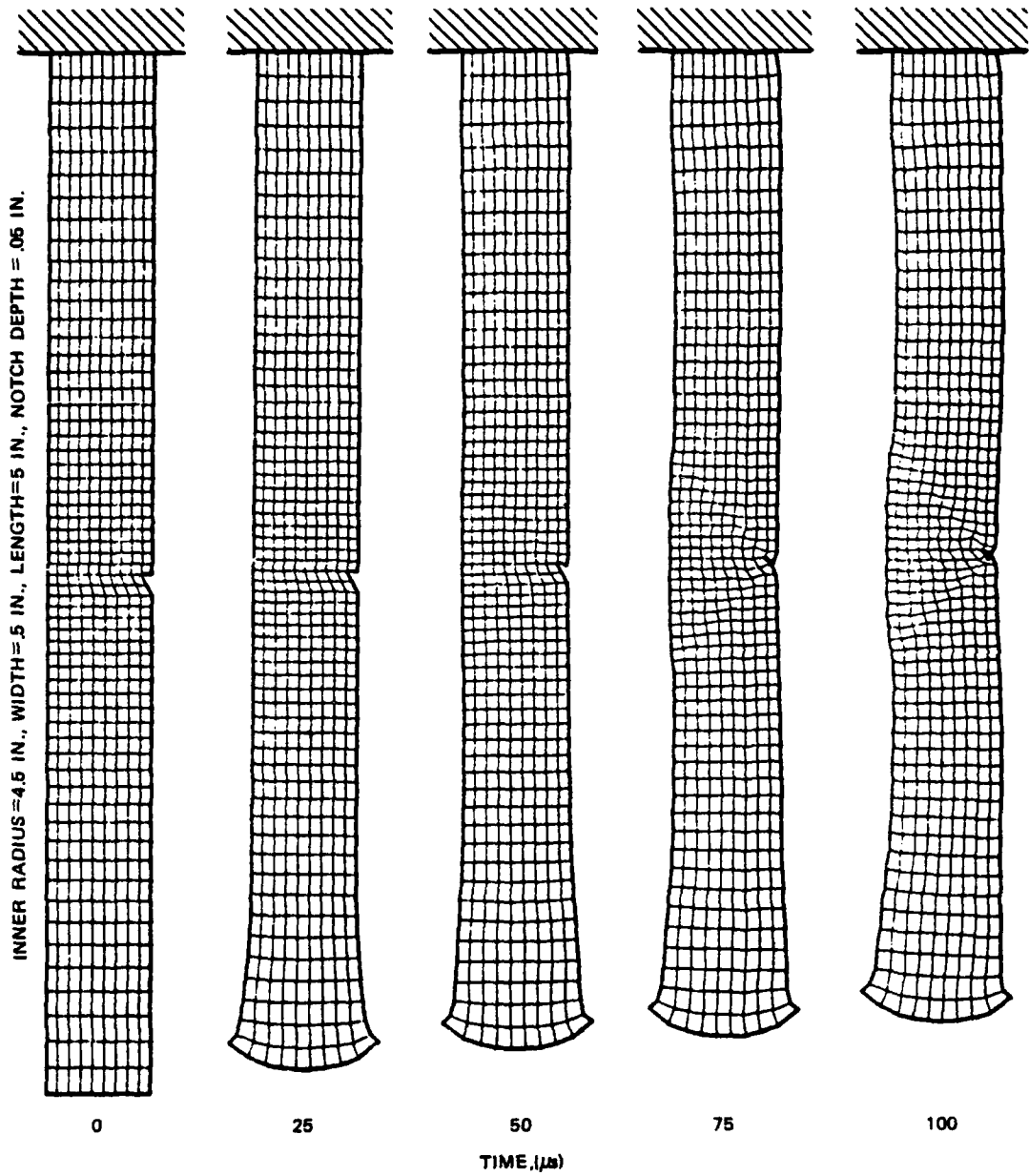


FIGURE 22. Grooved Case Segment, Groove on Outer Surface, Deforming in Response to Load C.

stages of case expansion following the detonation of the explosive.² Should the case survive, there may be cause to speculate as to the effect of the "presoftening" of the shear trajectories and on the partial or complete closing of the groove profile. It is possible that the groove profile could be designed to compensate for these effects if they should appear of consequence.

For sake of completeness, a finite element structure of a case segment with the groove located on the outside of the case wall was run against the deformation loading. Figure 22 shows that outside notches must generate stress patterns similar to inner grooves, with the yielding bands emanating inward from the groove position. A wedge-shaped torus is pushed into the warhead cavity. In any case, the presence of a groove can cause potentially significant deformations not seen by plain-wall cases. Whether these deformations result in case failure depends on the properties of the case material and on the duration of the load.

What kind of failure model should be used to predict the actual failure of the case depends on the results of experimental work. The finite element simulation indicates such a well-defined shear pattern that it may be possible to learn something quite useful by combining analytical and physical data. It would be a substantial contribution to formulate a failure model that could be used with confidence in warhead simulations.

DISCUSSION AND CONCLUSIONS

REDUCTION IN ENERGY ABSORPTION CAPACITY

Juvinall⁵ notes that stress raisers in a tensile bar subjected to impact loads produce two separate effects: (1) The reduction in cross section drastically reduces the energy absorption capacity; (2) The stresses in the plane of the groove are concentrated near to the surface of the groove. It might be expected that these effects would be similar to the behavior patterns of the grooved cylindrical segments under the compressive loads that were used in this study. Indeed, it has been shown qualitatively from the stress patterns caused by the presence of a groove that there is an initial concentration of yielding near the groove that then spreads out in 45-degree zones from the groove. One can use the idea of a reduction in energy absorption to make quantitative predictions of the effect of a groove on the breakup velocity of a projectile.

⁵ Robert C. Juvinall. *Stress, Strain, and Strength*. New York, McGraw-Hill, 1967. Chapter 9.

If the inner radius is denoted by R , the case thickness by t , and the groove depth by d , and if the groove is located at the center point of the cavity bulge, then a reduction in the failure velocity V_f could be expected as given in the equation

$$V_f(t) = V_f(0) \left(1 - \frac{d}{t}\right) \left(\frac{2R + d}{2R + t}\right) \quad (3)$$

This is based on the assumption that the kinetic energy of the warhead prior to impact that is needed to cause breakup is proportional to the energy absorption capacity of that segment of the case at which the warhead fails, that is, at the cavity bulge.

No generalization or simple calculation as Equation 3 can be given for the effects of a circumferential groove away from the center of the cavity bulge or when the warhead failure is due to front-end fractures that are sometimes associated with the perforation of steel plates, except that the reduction in breakup velocity should be smaller and, as a function of notch depth, more complex. There is a need for experimental work here.

Estimates can also be made for the additional wall thickness at the cavity bulge that is needed to compensate for the loss in energy absorption capacity due to the presence of a groove. If Δt is the addition to the wall thickness needed, then

$$\frac{(t + \Delta t - d)}{t(t + \Delta t)} \approx 1 \quad (4)$$

derived from straightforward algebraic manipulation. For $d \ll t$ this is satisfied for $\Delta t \approx 2d$. Of course, if the groove is not located at the cavity bulge, then no compensating thickness may be necessary since the case may not fail at the groove location.

SECONDARY FAILURE ZONE

Ductile Fracture

When the plane of the groove is located away from the primary failure zone, the results of the finite element simulations predict that a secondary failure zone will be created and that it will have a width of $2t$, twice the wall thickness. The width of the primary failure zone, based on the theory of buckling of thin-walled cylinders, is greater than $2\sqrt{R \cdot t}$, which for the radii and wall thicknesses of concern to this study is a figure greater than $4t$. Comparing the deflections obtained by the groove rings in the case deformation simulations with cavity bulge deflections obtained analytically and experimentally by Stronge and Schulz for similar times,⁴ it is doubtful that if the failure is

ductile that the secondary failure zone would become the point to initiate breakup. This is because the primary failure zone absorbs energy before the secondary zone and because the primary zone is bigger than the secondary zone, deforming more as a hinge than as an expanding ring which better characterizes the deformation in the groove region.

Brittle Fracture

If breakup is initiated by a brittle fracture, then the secondary zone may be the region of initial failure. Experiments by Papirno, Mescall, and Hansen⁶ with solid cylinders of 4340 steel impacting semi-infinite steel targets show a transition in failure mode at a Rockwell hardness of C 44, failing by ductile fracture below this hardness and by brittle fracture above. However, since a Rockwell hardness of C 46 is marginal for use in a shear-control system and C 60 unacceptably brittle (see Table 1), one might justifiably expect that there would normally be no problem of a brittle fracture originating at the groove. Thus, while it may be of little importance for predicting effect of a shear-control grid on the survivability of an impacting warhead, it could be of use in the development of a more general failure model to investigate the effect of hardness on the failure mode of circumferentially grooved cylinders.

EXPERIMENTAL EVIDENCE

Subsequent to this analytical study, test firings of circumferentially grooved projectiles against steel plate and simulated concrete targets were conducted by Schulz and Heimdahl.⁷ The projectiles were sectioned and examined. A brief description of the results of this work may be beneficial at this point.

The appropriateness of Equation 3 for estimating the effect on the breakup velocity of a circumferential groove located at the cavity bulge for a projectile penetrating simulated concrete was confirmed as the equation provided a good fit to the experimental data. (The same projectile did not fail at the cavity bulge when impacting the steel plates and so Equation 3 had no meaning.)

⁶ Army Materials and Mechanics Research Center. "Beyond the Taylor Test to Fracture," by Ralph P. Papirno, John F. Mescall, and Anna M. Hansen, in Proceedings of the Army Symposium on Solid Mechanics, 1980, *Designing for Extremes: Environment Loading and Structural Behavior*. Watertown, Mass., AMMRC, 1980. (AMMRC MS 80-4, pp. 367-385, publication UNCLASSIFIED.)

⁷ Naval Weapons Center. *Survivability of Penetrators With Circumferential Shear-Control Grooves*, by J. C. Schulz and O. E. R. Heimdahl. China Lake, Calif., NWC, April 1981. (NWC TP 6275, publication UNCLASSIFIED.)

The existence of the bands of yielding emanating at 45 degrees from the root of the groove has been established by metallographic examination of the sectioned projectiles under oblique lighting.⁸ The zones in which plastic work was accomplished has an outline similar to the outline of the bands of yielding calculated by the finite element code. The characteristic deformation pattern or groove ring is evident in the sectioned and non-sectioned projectiles and is similar to the patterns generated by HONDO II for this study.

Some of the 45-degree yielding bands in the test projectiles contained parallel shear bands and fracturing. An unexpected result was the presence of a tensile fracture originating at the root of the groove and running radially across the width of the zone of plastic work. These fractures may occur during unloading (perforation of the plates or rebounding in the simulated concrete) as they do not occur simultaneously with a shear fracture.

SUMMARY

Extending the results of this study of a warhead case with a circumferential groove to warheads with shear-control grids must be done with caution. However, the following conclusions are supported:

1. The presence of a shear-control grid may be detrimental to the survivability of an impacting warhead by reducing the breakup velocity. This will be especially evident if the grid is present in the primary failure zone.
2. The detrimental effects of a shear-control grid can be reduced by minimizing the depth of the groove profiles, or, alternatively, by increasing the case thickness. (This may not be practical in many instances.)
3. The detrimental effects of a shear-control grid can be reduced by increasing the distance from the nose to the grid, and possibly can be eliminated completely by keeping the grid out of the primary failure zone.

⁸ J. C. Schulz, J. Pearson, O. E. R. Heimdahl, and S. Finnegan. "Effect of Shear-Control Grids on the Survivability of Penetrator Warheads," in *Proceedings of the Sixth International Symposium on Ballistics, Orlando, FL., Oct. 1981*, pp. 232-240. American Defense Preparedness Association, publication UNCLASSIFIED.

Conclusions of this finite element study specific to the effect of circumferential grooves on the survivability of impacting warheads are:

1. A circumferential groove causes yielding patterns not evident in a plain-wall case. The stress distribution depends on the depth and location of the groove.

2. For a grooved case under a sufficiently high compressive load, bands of yielding grow from the groove position across the width of the case. If the load is of sufficient duration as well as intensity, a secondary failure zone or groove ring with width approximately twice the wall thickness will be evident on the case. The deformation can be characterized as the displacement of a right-triangular cross-sectioned torus with vertex at the groove root being pushed away from the groove.

3. The growth history of the bands of yielding depends on the distance of the groove from the plane of loading, on the depth of the groove, and on the duration of the load, and is independent of the groove orientation and profile.

4. The reduction in breakup velocity for an impacting warhead with a circumferential groove located in the plane in which the plain-wall warhead fails is a function of groove depth. Equation 3 may be appropriate in many instances for calculating this reduction. THE REDUCTION IN BREAKUP VELOCITY IS REDUCED OR ELIMINATED ENTIRELY IF THE GROOVE IS MOVED OUT OF THE PRIMARY FAILURE ZONE.

INITIAL DISTRIBUTION

- 10 Naval Air Systems Command
 - AIR-00D4 (2)
 - AIR-3021 (2)
 - AIR-350 (1)
 - AIR-350D (1)
 - AIR-512 (1)
 - AIR-533 (1)
 - AIR-541 (2)
- 5 Chief of Naval Operations
 - OP-03 (2)
 - OP-05 (1)
 - OP-098 (1)
 - OP-55 (1)
- 1 Chief of Naval Material
 - MAT-08L (1)
- 7 Naval Sea Systems Command
 - SEA-62R (5)
 - SEA-99612 (2)
- 4 Chief of Naval Research, Arlington
 - ONR-102 (1)
 - ONR-461 (1)
 - ONR-473 (1)
 - ONR-474 (1)
- 1 Air Test and Evaluation Squadron 5
- 1 David Taylor Naval Ship Research and Development Center, Bethesda
- 1 Fleet Anti-Air Warfare Training Center, San Diego
- 1 Marine Air Base Squadron 32, Beaufort
- 1 Marine Corps Air Station, Beaufort
- 1 Naval Air Engineering Center, Lakehurst
- 1 Naval Air Force, Atlantic Fleet
- 2 Naval Air Force, Pacific Fleet
- 1 Naval Air Station, North Island
- 2 Naval Air Test Center (CT-176), Patuxent River (Aeronautical Publications Library)
- 1 Naval Avionics Center, Indianapolis (Technical Library)
- 1 Naval Explosive Ordnance Disposal Technology Center, Indian Head
- 1 Naval Ocean Systems Center, San Diego (Code 131)
- 1 Naval Ordnance Station, Indian Head (Technical Library)

NWC TP 6288

- 1 Naval Postgraduate School, Monterey
- 5 Naval Surface Weapons Center Detachment, White Oak Laboratory,
Silver Spring
 - WR-13, R. Liddiard (1)
 - J. Erkman (1)
 - Dr. S. Jacobs (1)
 - Guided Missile Warhead Section (1)
 - Technical Library (1)
- 1 Office of Naval Research Branch Office, Chicago
- 1 Office of Naval Research Branch Office, Pasadena
- 1 Office of Navy Technology, Arlington (MAT-07)
- 1 Operational Test and Evaluation Force, Norfolk
- 1 Pacific Missile Test Center, Point Mugu (Technical Library)
- 1 Army Armament Materiel Readiness Command, Rock Island
(DRSAR-LEP-L, Technical Library)
- 4 Army Armament Research & Development Command, Dover
 - DRDAR-LCU-SS, J. Pentel (1)
 - Technical Library (3)
- 1 Aberdeen Proving Ground (Development and Proof Services)
- 3 Army Ballistic Research Laboratories, Aberdeen Proving Ground
 - DRDAR-SEI-B (1)
 - DRDAR-T, Detonation Branch (1)
 - DRDAR-TSB-S (STINFO) (1)
- 1 Army Material Systems Analysis Agency, Aberdeen Proving Ground
(J. Sperrazza)
- 1 Army Research Office, Durham
- 1 Harry Diamond Laboratories, Adelphi (Technical Library)
- 1 Radford Army Ammunition Plant
- 1 Redstone Arsenal (Rocket Development Laboratory, Test and
Evaluation Branch)
- 1 Rock Island Arsenal
- 1 White Sands Missile Range (STEWS-AD-L)
- 1 Yuma Proving Grounds (STEYT-GTE, M&M Branch)
- 1 Tactical Air Command, Langley Air Force Base (TPL-RQD-M)
- 3 Air Force Armament Division, Eglin Air Force Base
- 1 Air University Library, Maxwell Air Force Base
- 1 554th Combat Support Group, Nellis Air Force Base (OT)
- 2 57th Fighter Weapons Wing, Nellis Air Force Base
 - FWW/DTE (1)
 - FWW/DTO (1)
- 1 Tactical Fighter Weapons Center, Nellis Air Force Base (CC/CV)
- 1 Defense Nuclear Agency (Shock Physics Directorate)
- 12 Defense Technical Information Center
 - 1 Weapons Systems Evaluation Group, Arlington
 - 1 Lewis Research Center, NASA, Cleveland
 - 1 Arthur D. Little, Inc., Cambridge, MA (W. H. Varley)
 - 1 California Institute of Technology, Jet Propulsion Laboratory,
Pasadena (Technical Library)

2 Hercules Incorporated, Allegany Ballistics Laboratory, Cumberland, MD
1 IIT Research Institute, Chicago, IL (Document Librarian for
Department M)
2 Johns Hopkins University, Applied Physics Laboratory, Laurel, MD
(Document Library)
2 Johns Hopkins University, Applied Physics Laboratory, Laurel, MD
(Chemical Propulsion Information Agency)
1 Los Alamos Scientific Laboratory, Los Alamos, NM (Reports Library)
1 Princeton University, Forrestal Campus Library, Princeton, NJ
1 Stanford Research Institute, Poulter Laboratories, Menlo Park, CA
1 The Rand Corporation, Santa Monica, CA (Technical Library)
1 University of California, Lawrence Radiation Laboratory, Livermore, CA
1 University of Denver, Denver Research Institute, Denver, CO
1 University of South Florida, Tampa FL (Department of Structures,
Materials, and Fluids, W. C. Carpenter)